BNL-27976

EFFECTS OF IRRADIATION AND MECHANICAL STRESS ON THE SUPERCONDUCTING PROPERTIES OF CANDIDATE MAGNET CONDUCTORS

C. L. Snead, Jr. and Thomas Luhman
Metallurgy and Materials Science Division
Brookhaven National Laboratory
Upton, New York 11973

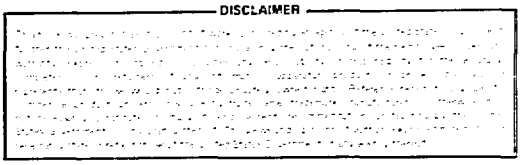

EFFECTS OF IRRADIATION AND MECHANICAL STRESS ON THE SUPERCONDUCTING PROPERTIES OF CANDIDATE MAGNET CONDUCTORS*

C. L. Snead, Jr. and Thomas Luhman
Metallurgy and Materials Science Division
Brookhaven National Laboratory
Upton, New York 11973

ABSTRACT

The effects of radiation damage on the superconducting critical properties of candidate magnet materials are reviewed. Neutron, and charged-particle irradiation results are covered. The discussion is restricted to effects in NbTi and the A15-compound superconductors. The utility of these conductors in radiation fields is first explored by defining the magnitude of critical-property changes with the fluence of various irradiating particles. The physical mechanisms that couple the irradiation defects to the observed critical-property changes are discussed. Annealing/recovery data on irradiated materials are included where they pertain to the understanding of the physical mechanisms involved, and thereby to the desirability of magnet annealing in actual operating circumstances. Although among the A15 compounds Nb_3Sn is now the leading candidate for high-field magnet applications, results for other A15 compounds that appear to be fabricable as conductors will also be covered. The general conclusions to be drawn for A15's and NbTi operating in a fusion-magnet configuration are that total fluences on the order of a few $x10^{18}$ n/cm^2 over the life of the magnet offers no serious problem to the magnet's properties. Annealing NbTi to room temperature is beneficial, annealing the A15's is detrimental. The fluence limits are for the entire magnet, spots of higher fluence resulting from lesser shielding being not tolerable. The effects of both tensile and bending stresses on the properties of Nb_3Sn filamentary conductors are also surveyed. Some new data on the synergism

---

*Work performed under the auspices of the U.S. Department of Energy.

between irradiation and stress effects are also presented. The results are discussed in terms of materials limits in application, and also in terms of possible ways new fabrication techniques may extend the range of strain that is both tolerable and beneficial.

I. Introduction

Many factors are involved in the choice of materials for magnets to be used in fusion devices employing magnetic confinement. The economics of producing large volumes of high field strengths dictate first of all the superconducting are required. The field strength required then sets constraints on the critical properties of the superconductor that are necessary for that field. Into the choice of material must then be factored whether or not that material can be fabricated into a conductor with which the magnet can be made. Although not a big consideration for experimental and demonstration reactors, the availability of specific materials in quantity can be of concern. Complicating this choice are the considerations of the environment in which the fusion reactor magnet must operate. By the very production of the required field strength, large hoop stresses are produced on the magnet which can be transmitted to the conductors. The response of the conductor to strain is then a factor to be considered. Likewise, the presence of an energetic neutron flux at the magnet site introduces the need for a knowledge of the radiation response of the conductor into the materials' choice process. In order to develop a complete understanding of the magnet's operating characteristics, synergistic effects such as the influence of radiation effects on the stress/strain behavior, and vice versa, are also needed.

We limit our discussion to two superconductors; NbTi and the A15 compounds. The response of NbTi to both irradiation and stress will be treated. We will be concerned with the same effects in the A15's, focussing our attention there on the prime candidate material, Nb_3Sn. We will examine this response with

an eye toward establishing "material limits" for both operation in a radiation field over a period of time, and for upper limits of allowable strain. The former has ramifications in the initial design considerations of, say, the amount of shielding that is needed, while the latter has direct bearing on the engineering design of the magnet itself. The discussion of these effects will wherever possible include the microscopic physical mechanisms which couple the change in state of the superconducting material to the change in critical properties observed. Finally, we will present some new data that for the first time examines one of the interactions between radiation and stress effects in Nb_3Sn.

II. NbTi

A. Irradiation Effects

The initial irradiation effects work in elemental type-II superconductors showed that T_c was a relatively insensitive property to damage.[1] Reductions of only a few tenths of a degree for various high-fluence irradiations were the rule. These reductions were attributed to the reduction of the superconducting gap anisotropy. In many of these irradiations it was noted that the reduction in T_c was not a single-valued function of the resistivity increase. Following low-temperature irradiation and subsequent annealing, the recovery of the T_c changes did not retrace the initial changes in a plot of ΔT_c vs. the resistivity change.[2] The conclusion was that the resistivity due to self-interstitials was a factor of 50 more effective in effecting T_c reductionsthan was resistivity due to other defects. The response of the upper critical field H_{c2} to damage followed a linear dependence with increasing normal-state resistivity as predicted by theory.[3]

The behavior of the critical-current density I_c with radiation, however, was not so straightforward. Ullmaier et al.[4] demonstrated that low-temperature electron and neutron irradiations to essentially equivalent resistivity

increases in niobium produced drastically different results on I_c. There was almost no change (a small increase) for the electron case, but for the neutron case a significant I_c increase (factor of 2). In addition, a "peak" in the plot of pinning force F_p ($=I_c H_\perp$) vs. applied field was found near H_{c2}. These two different responses to irradiation were again attributed to the differing nature of the damage created by the two different types of irradiation. The Frenkel-pair damage induced by the electron irradiation is not of sufficient size to act as pinning points for the fluxoids, whereas the larger cascades produced by the neutron damage are. The general result of defects on the critical current is then an increase of I_c due to increased flux pinning.

The radiation response of NbTi is somewhat more complicated than that for the elemental type-II superconductors. NbTi is a bcc random alloy with the Ti concentration in the range of 30-60 at.% for "commercial" conductors. Similar to the results in pure Nb, radiation damage of all types that have been investigated have only resulted in reducing T_c by a few tenths of a degree below the bulk value of ~9 K. The upper critical field of NbTi is paramagnetically limited to a value near 11.5 T and this value to first approximation is independent of the normal-state resistivity, and as a consequence independent of damage. There may, however, be second-order effects coupling resistivity to H_{c2}, but these have not been investigated to date in sufficient depth.

The response of I_c to damage depends mainly on the initial value of the critical-current density. This factor, in turn, is dependent mainly on the dislocation cell-wall density; i.e., an increasing pinning and I_c with increasing cell-wall density.[5-9] Early damage studies with low initial critical-current density specimens showed increased critical currents for heavy-particle irradiations. Söll et al.[5] for neutron damage induced at 4.6 K showed that for initial current densities J_{co} below ~1.7×10^4 A/cm^2 (measured at 4 T) increases in I_c resulted for fluences up to 3.6×10^{18} n/cm^2 (E > 0.1 MeV).

For higher-J_{co} specimens, only decreases in I_c were observed for all fluences. The increases in I_c for the low-current-density material can be explained by the same mechanism responsible for the increases observed in the pure Nb. The flux lines of the NbTi are not "optimally" pinned because the cell-wall spacing is too large, so that the defects introduced by the radiation are effective additional pinning sites, thereby tending to raise the critical current toward its optimal value.

For the samples with higher dislocation cell-wall densities the explanation for the I_c changes observed due to radiation are more involved. In this realm there is a competition between two radiation effects, one that tends to raise I_c (increased pinning sites), and one that decreases I_c. The reduction of the critical current in NbTi following 5 K reactor irradiation was demonstrated for specimens having initially high values of J_{co} ($\sim 1 \times 10^5$ A/cm^2 at 4 T).[10] These results are shown in Fig. 1. Measurements of the critical current density as a function of applied field are plotted for fields up to 3 T. The data labeled *a* represent the unirradiated values. Curve *b* shows the results after a neutron fluence of 3.2×10^{18} n/cm^2 ($E > 0.1$ MeV). Further reductions are shown in curve *c* where the final fluence was 7.5×10^{18} n/cm^2. The total degredation of the critical current near 3 T is seen to be ~40%.

One extremely suggestive phenomenon is seen in curves *d* and *e* where the specimens are annealed following the high-fluence irradiation to 100 and 270 K, respectively. Recovery of the J_c degradation is found during this annealing with ~60% recovery observed following the room-temperature anneal. Söll et al.[10] explained the J_c reductions as due to a weakening of the pinning strength of the dislocation cell walls due to the new pinning sites introduced into the cell cores by the irradiation. The recovery that is observed in annealing to room temperature, however, argues that at most Frenkel-pair and small cluster damage may be recovering, but at these low temperatures one would

not expect to produce recovery of defects of the size needed to produce pinning centers. The J_c reduction mechanism that has hence evolved does invoke a reduced pinning strength of the cell walls, but through a "magnetic" interaction rather than through a mechanical pinning interaction.

Dew-Hughes and Witcomb[11] have calculated the pinning force F_p of a cell wall and find that it depends upon the change in the Ginzburg-Landau factor κ in going from the cell interior across the cell wall. They get $F_p \alpha \Delta\kappa/d^3$ where d is the mean distance between cell walls. Since κ can be expressed in terms of the normal-state resistivity ρ_n of the material by the relation $\kappa = \kappa_o \pm A\gamma^{1/2}\rho_n$, where κ_o is a constant and γ is the electronic specific-heat coefficient, the change $\Delta\kappa$ is related simply to a change in the normal-state resistivity. Given the already tangled nature of a dislocation cell wall, one would then expect the result of irradiation to raise the resistivity of the cell core a greater amount than of the wall. This results in a net decrease in the $\Delta\kappa$ between the cell walls and cores and thereby reduces the pinning force of the walls. This is depicted schematically in Fig. 2.

The 100 and 273 K annealing results (curves d and e) of Fig. 1 give added credence to this interpretation. The percentages of J_c recovery observed correspond exceedingly well with the percentages of recovery in the change in normal-state resistivity induced by low-temperature neutron irradiation and annealing of NbTi done by Brown et al.[12] They found 40% recovery at 100 K and 70% recovery at 290 K. The irradiation-induced degradation of J_c in high-J_{co} NbTi seems best explained, then, through a reduction of the dislocation cell wall pinning strength due to the presence of Frenkel-pair damage in the cell cores.

Consistent with the well-known phenomenon of saturation of resistivity with high-fluence irradiation, the degradation of the critical current also

approaches a saturation value at high fluences. Fig. 3 shows the results of two different types of irradiation on the reduction of the critical current I_c/I_{co}.[13-15] The open circles are for ambient reactor irradiations (measured at 4 T), and the solid circles for 4.2 K irradiations using 30-GeV protons (also measured at 4 T). The saturation value of 20% total degradation is clearly demonstrated in the neutron case. The proton irradiations were not carried to sufficiently high fluences to establish a saturation value, although the beginning of an upward turning of the curve may be seen. The value for the saturated decrease in I_c may very well be different for irradiations at 4.2 K and higher temperatures. The amounts of I_c reduction and the saturation value may also be different for different compositions of NbTi. Sekula[16] has tabulated degradation and recovery effects in NbTi. One of the conclusions one can draw from the comparisons therein is that for nominally the same composition, Nb-66 at.% Ti. Söll et al. observed a 50% decrease from low-fluence neutron irradiation at 5 K, but Snead et al. found saturation at 20% degradation for high-fluence neutron irradiation at ~100°C. Whether this difference is attributable to the different temperatures of irradiation, or to the fact that Söll's specimens had the copper removed baring the NbTi filaments and the others had the stabilizer present, is, at present, an open question. Couach et al.[17] observed a 25% reduction of I_c for 10^{19} n/cm^2 at 77 K. Unfortunately, the Nb to Ti ratio was not specified. All other work reported for all temperatures of irradiation and NbTi compositions has produced total I_c reductions less than 20%.

We conclude that radiation damage decreases T_c of NbTi insignificantly. The effects of damage on H_{c2} have been found to be slight (owing to paramagnetic limitation effects), but no thorough study of this critical property has been made. The effects of irradiation on I_c are of more concern. For currently available NbTi conductors with J_{co} approaching 2 x 10^5 A/cm^2 at 4 T, degradation of I_c is directly related to the damage-induced increase of the normal-state

resistivity. Since ρ_N saturates at high fluences, the reduction of I_c should also saturate. For room-temperature irradiations, this saturation point has been found to be at the 20% reduction level. Whether there is a higher saturation level for lower-temperature irradiations is a possibility and very much an open question. From all low-temperature irradiations with both neutrons and energetic charged particles, the recovery of the degradation of I_c with annealing to room temperature has been consistent with the recovery of the increase of the normal-state resistivity induced by the damage. From an operational point of view for magnetically confined fusion reactors this means that between 50 and 70% of the critical-current degradation induced by helium-temperature neutron damage can be recovered by annealing the magnet to room temperature. Furthermore, it has been indicated that the more frequent these annealings over the irradiation lifetime of the magnet, the greater will be the total recovery, resulting in a minimum of damage accumulation.[13]

B. Stress/Strain Effects

Two aspects of the strain tolerances of NbTi conductors are considered; their mechanical behavior, and the response of the critical current to applied strain. Much of the recent work on multifilamentary NbTi conductors has centered on their mechanical strengths and the effects of stress and strain on superconducting critical current.[18-25] The conductors are composite materials consisting usually of twisted NbTi filaments in a Cu and/or a Cu-Ni matrix. Their composite character, strong filaments in a ductile metal matrix, leads to ultimate tensile strengths, UTS, which are attractively high [about 10^9 N/m^2 ($\sim$145 psi) for typical NbTi:Cu composites].

The effect of temperature on the UTS and percent elongation for NbTi:Cu composite is shown in Fig. 4.[18] This composite has a rectangular Cu matrix (Cu:NbTi = 2.8:1) containing 18 filaments of Nb-26% Ti, each has a nominal dia-

meter of 0.279 mm. The UTS increases nearly linerarly with decreasing temperature. Elongation increases to 77 K and then decreases to less than 2% of its original room temperature value. The decrease in elongation is unexpected. It has been proposed that the decreased elongation at 4.2 K is related to serrated stress-strain behavior often observed in NbTi composites at liquid-helium temperatures. A strain-induced martensite reaction has been invoked to account for the serrated behavior. According to this mechanism the Cu matrix of the composite restricts the extent to which the martensite develops thereby limiting the composite's low-temperature elongation.

Of importance with regard to mechanical properties is the observation of pseudoelasticity. Through pseudoelastic effects heat is generated and the critical current can be degraded. Pseudoelastic effects develop in the following way. Once strained such that the matrix exhibits plastic flow the elastic filament can, upon removal of the applied load, induce a compressive plastic strain in the matrix. With sufficient plastic deformation in the matrix pseudoelastic behavior, hysteresis loops, result. Stress-strain loops are unavoidable in large pulsed high-field magnets. In traversing such loops part of the work done results in heat generation and a large temperature rise can occur.[19] It has been estimated that heat produced if the pulse rate were 1 sec^{-1} would be 10^3 - 10^5 w/m^3 for a typical commercial NbTi conductor.[24] Even small changes in temperature can result in degradation of magnet performance since most large superconducting magnets operate near 5 K. For example, a typical design curve for the operation of a NbTi/Cu composite at 6 T would involve a current density J_c of 2 x 10^5 A/cm^2 at 4.2 K. This value is reduced to 2 x 10^4 A/cm^2 at 6.2 K.[26]

Figure 5 presents a J_c-strain relationship for a NbTi conductor.[22] The superconducting properties of NbTi solid solutions are relatively insensitive to small strains (less than ~1%). A degrading effect on I_c generally

begins at ~0.5% strain, and usually will only become appreciable after a few percent strain. Strains to near the composite's UTS, of the order of ~4.5%, lead to an I_c degradiation of ~30%. Such decreases in I_c are almost totally reversible, I_c returning to within 95% of its unstrained value when the applied stress is removed. The reason for critical current degradation with strain is not completely understood. Although the superconducting transition temperature T_c is decreased by a few tenths of a degree kelvin with applied strains, this is not sufficiently large to account for the observed decreases in J_c.[27] Ekin has proposed a possible mechanism envolving the generation of small defects, such as cracks, in the NbTi superconductors.[24] The size of the defects should be of the order of the superconducting coherence length, which for a Nb-45% Ti alloy is approximately 5.5 nm. As with any other mechanism, such as a martensitic transformation, the effectiveness of the defect in reducing critical current must be reversible with strain.

The influence of cyclic stress-strain on critical currents in NbTi composites is consistent with I_c measurements in unidirectional tests.[28] The following results were obtained by Fisher et al. on a ribbon composite containing 18 Nb-54% Ti twisted filaments in a Cu matrix, Cu:superconductor ratio, 2.7. For a maximum strain amplitude of 0.35% there was a decrease of 3% in critical current (4.0 T) during the initial 200 cycles. Increasing the maximum strain amplitude to 0.57% resulted in some current sharing between the filaments and the copper stabilizing material. Voltage occurred in an I_c-voltage plot when $I < I_c$. With cycling frequency exceeding 400 sec^{-1} and a maximum strain amplitude of 0.57%, voltage steps were observed at $I > I_c$. This latter effect was a function of magnetic field, disappearing when applied fields exceeded 4.0 T. Some recovery of the initial decrease in I_c occurred when the samples were warmed to room temperature, although in other tests on samples with increasing numbers of filaments this effect was less pronounced.

In summary, the multifilamentary NbTi conductors provide magnet builders with a reasonably strain-tolerant material. Both unidirectional and cyclic stress of the order of 1% produce only a few percent decrease in I_c. In most cases strains upwards of 4-5% produce only about a 30% degradation in I_c.

All of the results quoted above refer to strain tolerances at 4.2 K. The ductile NbTi alloys are quite strain tolerant at room temperature. In fact, an important mechanism for producing high critical-current densities in these alloys is the introduction by plastic deformation of dislocations.[29] Most experience to date indicates that NbTi conductors can be strained several percent during winding operations without noticeably affecting their subsequent performance at liquid-helium temperatures.[30]

III. A15 Compounds

A. Irradiation Effects

For fusion reactors requiring confinement field strengths greater than ~9 T, superconductors with critical properties superior to those of NbTi are required. At present only the A15 compounds not only have the requisite critical properties, but are also fabricable into usable conductor. When other considerations such as cost and material availability are also considered, Nb_3Sn emerges as the prime candidate material. In NbTi we saw that the effects of irradiation on the critical current was either through the generation of pinning centers, or by the alteration of the effectiveness of existing pinning centers such as by changing ρ_N. Changes in T_c in NbTi were negligible. In the highly ordered A15 compounds the situation is quite different. The A15 structure (A_3B) is highlighted by orthogonal but nonintersecting chains of A atoms parallel to the <100> directions. When the order along these chains is disrupted by such radiation-induced defects as vacancies, B atoms on the A sites, or static displacements due to off-line A atoms produced by local lattice distortions, large changes in T_c and subsequently all of the critical properties

take place. In fusion-reactor environments, where neutron fluences between 10^{18} and 10^{20} n/cm^2 over the life of the device can be realized, severe reduction in the long-range order may be expected.

Large reductions of T_c due to ambient reactor temperature neutron irradiations were first observed by Bett.[31] A fluence of ~5 x 10^{19} n/cm^2 (E > 0.1 MeV) reduced T_c from 18 to 5 K. This resulted in a reduction of I_c effectively to zero. Bett also observed that for low fluences where T_c changes have not become significant and for magnetic fields above ~2 T that there was an increase in I_c with fluence. Recovery of the T_c changes was accomplished by annealing the specimens to 900°C. Sweedler et al. (see Fig. 6) irradiated several A15 compounds with neutrons at reactor ambient temperature to fluences of 5 x 10^{19} n/cm^2 (E > 1.0 MeV) and showed that the T_c reduction with fluence was a common phenomenon to the A15s.[32-37] Mo_3Os was an exception in that at the highest fluences T_c had not reduced to below 4.2 K. This resulted in the observation that if the B atom is a transition element its taking the place of a transition-element A atom (Nb or V), its effect on changing the electronic properties of the A chain through a change in long-range order is much smaller than that of a non-transition metal.

There have been several annealing studies of A15 compounds neutron irradiated at ambient reactor temperature. The general results show that recovery (as measured by increasing T_c) takes place in the same temperature range that has been associated with self- or interdiffusion in the A15. This temperature has been established from single and multifilamentary A15 wire fabrication using the "bronze technique". For Nb_3Sn this temperature is 700°C[36] and 400°C[38,39] for V_3Ga. Essentially no recovery is observed until this recovery stage is reached. This recovery stage is attributed to reordering of the A15 structure, especially the A chains, and is controlled by self-diffusion in the A15 compound.[35,40-42] The microscopic mechanism(s) of vacancy diffusion in the A15 system is at present conjectural.

The recovery of T_c suppressions following cryogenic-temperature irradiations is somewhat more complex. Brown et al.[43] irradiated Nb_3Sn films at 20 K to a fluence of 1.3×10^{18} n/cm^{-2} (E > 0.1 MeV) and observed a depression of T_c from 17.85 to 16.7 K, and an increase of 4.3 μΩcm in the normal-state resistivity (see Fig. 7). Two recovery stages were observed, a small one at ~100 K and a larger one beginning at ~270 K and extending up to 500 K (see Fig. 8). For this annealing range there was a recovery of $\Delta\rho_N$ of 21% and a recovery of ΔT_c of 43%. In terms of the model of T_c reduction where disorder on the A chains is responsible for a reduction of the electronic density of states and thereby T_c, the recovery can be explained in terms of interstitial migration at the lower-temperature stage, and vacancy-migration in the broader high-temperature stage. The interesting thing here is that the higher percentage of recovery of T_c relative to $\Delta\rho_N$ indicates that vacancies on the A chains contribute significantly more to the reduction of T_c per defect site than do B atoms occupying A sites (disorder). This is conceptually appealing, however, within the model where the density of states is determined by the A atom electronic overlap, and then considering the effects of neighboring A-atom relaxation into the vacancy. This includes relaxation effects not only on the affected chain, but also for adjacent chains.[44] Occupation of the defect site instead by a B atom would somewhat mitigate this relaxation. The remaining $\Delta\rho_N$ after the 500-K anneal is then interpreted as resistivity due to the A - B interchange disorder in the sample and the remaining ΔT_c as due to this disorder.

The preceding has described the T_c reduction and recovery for low-fluence low-temperature damage (ρ_N following irradiation was 20.8 μΩcm whereas the saturation ρ_N for Nb_3Sn is 127 μΩcm). For irradiations at higher fluences, less recovery in ΔT_c is observed. Brown et al. in the same experiments discussed above also irradiated uranium-doped Nb_3Sn which produced an accelerated

damage rate through the production of fission fragments. The specimen was irradiated until saturation was reached in the normal-state resistivity which resulted in a T_c just below 4 K. Annealing this specimen to 425 K produced no recovery in either $\Delta\rho_N$ or in ΔT_c. It is apparent that the resistivity contribution of the disorder in this case is far greater than that of the Frenkel-pair damage as to make the recovery of the latter inconsequential. We thus have two fluence regimes of differing recovery behavior: the low-fluence regime (up to a few 10^{18} n/cm^2) where some recovery is observed since the Frenkel-pair resistivity is a considerable part of the total resistivity change, and the high-fluence region where the resistivity due to disorder is much greater than that of the Frenkel-pairs, and no recovery is seen without going to several hundred degrees centigrade. For irradiations at room temperature and above, only the contribution due to disorder will be present.

With an understanding of the response of T_c with fluence and of the mechanisms coupling the defect state to the observed property changes, a good platform is provided to investigate the effects of irradiation on the other critical properties.

We saw that in NbTi that the response of I_c to irradiation depended strongly on the initial critical current density of the material. Low-J_{co} material exhibited increased I_c with radiation and was interpreted as due to increased pinning, whereas high-J_{co} material exhibited only degradation of I_c. In this respect Nb_3Sn behaves similarly. With the advent of "optimized" Nb_3Sn with critical-current densities on the order of 2×10^6 A/cm^2 at 4 T "engineering grade" material was available on which more-definitive information could be obtained. Schweitzer and Parkin,[45] Parkin and Schweitzer,[46] and Bett[31] showed that for fluences greater than 1×10^{18} n/cm^2 the I_c decreased quickly and a few 10^{19} n/cm^2 went to zero as measured at 4.2 K. This was seen as due to the degradation of T_c below 4.2 K due to the irradiation-induced anti-site disorder.

Brown et al.[47] have carried out an extensive series of investigations of low-field (< 4 T) and low-fluence (< 2 x 10^{18} n/cm^2) regime of neutron damage in Nb_3Sn at low temperatures. Below ~1.5 T they found that I_c decreased with fluence, but above that field I_c increased with increasing fluence. Annealing to 295 K resulted in the recovery of some of the higher-field enhancement, but little change for the lower-field degradation (see Fig. 9). The enhancement of I_c was also seen to be greater as the field was increased. This phenomenon of increased enhancement of I_c with increasing applied field was demonstrated by Snead and Parkin[48] for 100°C reactor irradiations and measurements up to 16 T. These results are shown in Fig. 10. From the measurements made at higher fields it became apparent that the increases in I_c at low fluence stemmed mainly from an increase in H_{c2}. These field-dependent increases in I_c are better shown in Fig. 11 where the reduced I_c is plotted vs. fluence with the applied field parametrized. This increase in H_{c2} is due to the increase of ρ_N through the expression $H_{c2} = A\, T_c\, \rho_N$. Thus, throughout the fluence regime up to ~2 x 10^{18} n/cm^2, ρ_N increases but T_c is relatively constant, and H_{c2} increases with increasing fluence. The increases seen in the work of Brown et al. are larger for a given fluence since the defect retention is larger at low temperatures than that at 100°C. The recovery of Frenkel-pair damage in the anneal to 295 K (Brown et al.,[43] Fig. 9) is then seen as responsible for the partial recovery of the increases in I_c observed by Brown et al.[47] The contribution to ρ_N following the room-temperature is then associated with antisite disorder, which has been shown to be recoverable only by annealing to ~700°C.

The I_c changes with irradiation in the low-field (below 3 T), even though more accessible experimentally, are less well understood than those at higher fields. The low-temperature irradiations of Brown et al.[47] clearly showed that only decreases in I_c are observed as a consequence of the neutron irradiation, and that these decreases are partially recoverable upon annealing

to room temperature (Fig. 9). This would argue that the decreases are attributable to some property of the Frenkel-pair damage just as the increases in I_c at the higher measuring fields are. This property for the high-field case was the normal-state resistivity. It is noteworthy that the crossover from low-field to high-field behavior (from decreases of I_c to increases of I_c at low fluences) occurs at just the point where the pinning force F_p has its maximum. This means that at that point the flux-pinning mechanism is shifting from flux-line pinning dominance to flux-line shear as the controlling mechanism.[49,50] It is then not unreasonable to expect that the former mechanism could depend upon the normal-state resistivity in a different way than the latter mechanism. The low-field response of I_c to damage could be controlled by the same mechanism that has been established for NbTi; namely, reduction of the dominant pinning site (here, grain boundaries) pinning strength because of an increase of ρ_N in the interior of the grains. Thus at low fields a reduction of I_c results from an increase of ρ_N, while at higher fields I_c increases with increasing ρ_N. Where the pinning force has its maximum no change in I_c occurs until T_c changes begin to be significant.

For higher fluences ($>2 \times 10^{18}$ n/cm^2, E > 1 MeV) the reduction of T_c drives H_{c2} down and thus I_c with it. The high-fluence portion of Fig. 11 demonstrates that the I_c reduction is field independent in the high-fluence regime. With increasing fluence, I_c tends to zero (measured at 4.2 K) as T_c tends toward ~3 K for Nb_3Sn. One is probably safe in assigning all of the change in J_c to the reduction of T_c in this high-fleuence regime. There are very few data for irradiations at low temperature and for annealing in this high-fluence regime. Söll et al.[51] neutron-irradiated Nb_3Sn diffusion wires to 4×10^{18} n/cm^2 (E > 0.1 MeV) at helium temperature. The 150% enhancement of J_c observed at 50 kG was almost completely recovered upon annealing to 250 K. Since increases, rather than decreases, in J_c were observed, one concludes that

the "high-fluence regime", where T_c changes dominate, had not been reached in this work.

There are no high-fluence low-temperature neutron results reported for J_c measurements in Nb_3Sn. Irradiations of high-J_{co} Nb_3Sn at low temperatures into the T_c-limited high-fluence regime have been performed using 30-GeV protons at the Brookhaven Alternating Gradient Synchrotron.[13,52] The damage-energy cross section for these particles has been estimated at $\langle E_D \rangle$ = 500 bkeV. Single and multifilament wire specimens were irradiated at 4.2 K and I_c measurements made in situ in fields up to 40 kG. Figure 12 depicts the results of an irradiation of commercial Airco 361-core wire. The irradiation was interrupted at 7 x 10^{17} p/cm^2, the specimen annealed to room temperature, and the irradiation continued to a total of 1.6 x 10^{18} p/cm^2. The previously discussed behavior of larger decreases at low field in the high-fluence regime is to be seen for this case also.

As with the specimens irradiated above room temperature with neutrons to high fluences, large decreases in I_c with fluence are observed. At 40 kG a 99% reduction of I_c has taken place for the 1.6 x 10^{18} p/cm^2 exposure. The important thing to note here is the lack of recovery of the specimen's I_c with annealing. Subsequent to the 7 x 10^{17} p/cm^2 segment, the specimens were annealed to room temperature and I_c then remeasured. The solid triangles show that within experimental uncertainty no recovery is observed. Similar annealing (data not shown) following the next irradiation segment to 1.6 x 10^{18} p/cm^2 produced values of I_c identical to those prior to this latter anneal. In contrast to Nb-Ti, then, we see that no recovery of decreases in I_c takes place in Nb_3Sn with room-temperature annealing. The damage responsible for the changes is antisite disorder and is not recoverable until several hundred degrees centigrade above room temperature.

Contrast in the degradation rate and recovery between Nb_3Sn and Nb-Ti for low-temperature irradiations is seen in Fig. 13. Here the relative decrease in I_c measured at 400 kG for two specimens irradiated simultaneously with 30-GeV protons is plotted as a function of fluence. The much faster degradation rate of the Nb_3Sn versus that of the Nb-Ti is immediately evident. The recovery of the I_c decreases is represented by the vertical movement of the data points at 0.7 and 1.6 x 10^{18} p/cm^2. The three points at the higher fluence represent the samples irradiated, annealed to 125 K, and then to 290 K. The lack of recovery in the Nb_3Sn specimen is the striking feature that contrasts sharply with the recovery behavior of NbTi.

For neutron damage in Nb_3Sn induced above room temperature we have seen that critical-current degradations and T_c reductions start becoming significant at the ~2 x 10^{18} n/cm^{-2} fluence level for neutrons E > 1 MeV. This corresponds to a damage energy of ~0.2 eV/atom.[15] According to most projections of accumulated fluence for fusion devices over a 10 - 30 year service period this fluence will only begin to be achieved at the magnet location at the endpoint of the service period. However, as it has been pointed out several times, this estimate assumes that the entire magnet is protected by the nominal shielding that is specified for the given device design under consideration, and for any areas of the magnet that do not enjoy the full effects of the shielding (hot spots), deleterious fluences might be achieved. Many such possible areas are neutral-beam-injection ports, vacuum accesses, etc. where the shielding geometry is not optimum. It will then be these spots of higher than average fluence that will ultimately determine the limiting value of the critical current for the entire coil of which they are part.

This "weak link" nature of a Nb_3Sn coil can be demonstrated in the microcosm of a short sample of Nb_3Sn filamentary conductor that has been nonuniformly irradiated along its gauge length for measuring T_c resistively. The solid line

in Fig. 14 is the voltage across the specimen as the temperature is swept through the normal-to-superconducting transition. The most vertical part at just above 16 K is produced by that part of the specimen that received none of the proton beam (30 GeV) and thus is part of the curve that depicts a totally undamaged specimen (showed by the dashed curve at 16 K). The solid curve indicates that the inhomogeneous fluence distribution resulted in the Nb_3Sn having T_c values ranging from 10.7 K at the highest-fluence area up to just above 16 K corresponding to undamaged material.

The critical current of the specimen was determined (measured at 4 T) and compared with results from reactor-neutron irradiations on similar wire specimens. From those irradiations the relationship between both T_c and I_c with fluence had been established, and the width of the T_c transition was observed to be independent of the amount of T_c reduction. By equating the I_c values for both the neutron and proton irradiations an equivalent T_c for the two treatments could be obtained. The equivalent neutron-damage T_c is plotted as the lower-temperature dashed curve of Fig. 14. Note that the low-temperature onset occurs at the same place for both the proton and neutron-irradiated specimens. This shows that the critical-current value of the proton-irradiated wire is determined by that part of the specimen that has received the highest fluence and therefore has the lowest T_c. The average fluence is not the important factor in determining the value of the critical current but rather the highest fluence on any part of the specimen.

Where the radiation shielding is effective, the neutron spectrum seen by the magnet will be somewhat softer than a fission spectrum, so fission-reactor simulation of neutron damage to the magnet is quite reasonable. Where the shielding is not as effective (hot spots), the spectrum will be much harder with a higher component of 14-MeV-neutron contribution. There has been some work on the investigation of the effects of high-energy neutron damage on the

superconducting properties of A15 filamentary wires. Among the first such studies[53] was the irradiation of 19-core Nb_3Sn wires with 14-MeV neutrons at the Rotating Target Neutron Source (I) at Livermore. Fig. 15 depicts the changes in I_c for these specimens for fluences up to 1×10^{18} and for test fields to 4 T. Note the decrease of I_c with fluence at low fields and the apparent crossover between 3 and 4 T, characteristic behavior noted for fission-reactor irradiation. Higher-field data are not available for these low-fluence irradiations.

Higher-field data are available[51] for the 1 and 2×10^{18} n/cm^2 fluences, however, and are shown in Fig. 16 along with similar measurements on fission-reactor irradiations to fluences that produce results that bracket those of the 14-MeV irradiations at the higher fields. The main conclusion to be drawn from this comparison is that the high-energy-neutron irradiation produced less I_c reduction at low fields than the High Flux Beam Reactor (HFBR) irradiations for high-field reductions that are comparable. This has been interpreted as being due to less resistivity increase per unit damage energy in the high-energy neutron case due to greater Frenkel defect recombination with the more extensive cascade and subcascade structures.[53] There is no compelling argument for the generation of direct pinning centers by either types of irradiation.

Scanlan and Raymond[54] irradiated single-core and multifilamentary Nb_3Sn at 4.2 K with 14.8-MeV and d-Be spectrum neutrons. The highest fluence reached was $\sim 8 \times 10^{20}$ n/m^2 for the former and $\sim 8 \times 10^{21}$ n/m^2 for the latter. For the 14.8-MeV irradiations, increases in I_c were observed to ~30% and were constant over the 8-12 T measuring range. The higher-fluence d-Be irradiations produced I_c increases of ~50%. Annealing to room temperature produced no measurable recovery in any of the cases. Comparison is made with the low-temperature fission-reactor irradiations of Brown et al.[47] Based upon damage-energy scaling, the 15% increases in the Nb_3Sn wires investigated by Brown et al.

appear to be larger than what would be predicted. On the other hand, scaling on the basis of large cascades (attributing all of the I_c change to flux pinning by cascades) overestimates the differences seen in the two types of irradiation. Based upon this analysis (admitting that the peak, or I_{max}, had not been reached for the fluences of either irradiation), a conclusion that possibly two mechanisms were at work, presumably pinning at cascades and increasing H_{c2} due to increasing ρ_N. The lack of recovery in the high-energy-neutron case in annealing to room temperature whereas the Brown et al. results did show recovery argues that possibly the cascade affects are more important in the high-energy case than for the fission-reactor neutron case.

B. Stress/Strain Effects

Nb_3Sn multifilamentary conductors are prepared by a unique solid-state diffusion technique called the "bronze-process". Long lengths of multifilamentary conductors are produced by drawing ductile composites consisting of niobium filaments in a bronze (Cu and Sn) matrix. Heat treating the wire composites (at temperatures ranging from 650 to 750°C) results in Nb_3Sn compound formation at the interfaces between the filaments and the matrix. A recent review of the metallurgy of bronze-processed conductors has been given in a book by Luhman and Dew-Hughes.[29]

Room-temperature stress-strain behavior of multifilamentary Nb_3Sn conductors can be divided into two distinct types.[55] Wires having more than ~16 volume percent niobium prior to compound formation exhibit plastic flow to ~1% and brittle failure at strains of 1 or 2%. An example of a stress-strain curve for this type of conductor is given in Figure 17 (type A).[55] When the initial volume fraction of niobium is less than ~16% plastic flow is again observed to ~1% strain. However, further straining will occur at nearly a constant applied load until ductile fracture of the matrix at strains of

~10%, note Fig. 17, (type B). For this latter type of conductor, experiments showed individual Nb_3Sn filaments failed at ~1% strain but the larger volume fraction of matrix material enables the conductor to hold together up to the higher strains.[56] For each type of conductor the mechanical properties are, in general, not dependent on any remaining small amounts of unreacted niobium. The Nb_3Sn filaments fail from 1 to 1.5% strain depending on the exact volume ratio of matrix to filament. This failure strain value is substantially higher than the breaking strain of 0.2% for arc-melted Nb_3Sn. Enhancement of Nb_3Sn failure strains in the filaments over that for arc-melted material is related to the composite nature of multifilamentary conductors. Factors such as residual strain in as-reacted conductors play an important role and are discussed below.

A question arises; how does the critical current of a Nb_3Sn conductor vary in the range of strain below the filament fracture value? It is essential to know, for example, if the critical current is degraded in any way by applied strains less than the failure strain. To answer this question, it is necessary to understand the state of residual strain existing in as reacted conductors. Owing to the relatively larger thermal contraction coefficient of bronze over niobium and Nb_3Sn the filaments in a multifilamentary conductor are subjected to a compressive strain upon cooling from the reaction heat-treatment temperature. This residual compressive strain on the Nb_3Sn decreases I_c in as-reacted conductors. With the application of externally applied tensile strains the residual compressive strains are counterbalanced and I_c increases towards a nearly strain-free value. As a result of this interaction between residual and applied tensile strains the critical current reaches a maximum when the two strains compensate each other. Straining beyond this point increases I_c in accordance with its functional dependence on tensile strain. The requirement for counterbalancing residual compressive strains therefore provides a mechanism by which the conductor's total strain tolerance is increased. A measure of the internal residual strain may

be obtained from an in situ, 4.2 K, I_c-tensile strain measurement. The value of applied tensile strain corresponding to the maxima in an I_c-tensile strain plot is regarded as a measure of the internal residual compressive strain, ϵ_m.

Figure 18 presents I_c—tensile-strain data taken at 4.2 K and 4.4 T, for variously heat treated Nb_3Sn multifilamentary conductors as well as data for a multifilamentary NbTi conductor.[57,58] Table 1, after reference 57, gives pertinent characteristics of these conductors. Note the absence of a maximum in Fig. 18 for the NbTi conductor. For all Nb_3Sn curves I_c/I_{co} increases with strain and passes through a maximum at ϵ_m. One factor influencing the strain value associated with the maxima is the volume ratio of Nb_3Sn to bronze, see Table 1. By a force balance, as the relative amount of matrix to Nb_3Sn increases, the compressive strain induced in the Nb_3Sn increases. This has the effect of shifting the maximum values of I_c/I_{co} toward higher applied strains. Another factor affecting ϵ_m is the flow stress of the bronze. The flow stress decreases with longer reaction heat treatment times owing to Sn depletion as the Nb_3Sn volume fraction grows. Sn depletion softens the bronze which undergoes plastic deformation during cooling from the reaction heat-treatment temperature. Since it is during this cooling step that the compressive strain is induced in the Nb_3Sn filaments, any plastic flow in the bronze during cooling leads to a decrease in the induced compressive strain. In commercial conductors with bronze-to-filament ratios less than 3, Sn depletion of the bronze can be nearly 100% in the fully reacted condition and softening of the bronze can be a major factor in reducing ϵ_m.

I_c data in Fig. 18 exhibit parabolic curvature. Normalizing by the current at the maximum I_c yields[58]

$$I_c = I_{cm}/(1 + C|\epsilon_o|^n)$$

where ε_o is the intrinsic strain defined as $\varepsilon_o = \varepsilon - \varepsilon_m$ (the filaments are under compressive strains when $\varepsilon_o < o$ and tensile strains of $\varepsilon_o > o$). The best-fit parameters are $n = 1.92$ and $C = 3350$. Quadratic curvature is not always observed and it appears that some effort is still required before the functional dependence of I_c is well understood in terms of theory.[59]

Another aspect of I_c-strain behavior at applied strains less than the fracture strain has to do with reversibility of I_c when the applied load is removed. Figure 19 presents critical-current data for a 2869-filament, bronze-processed, Nb_3Sn conductor as a function of both total and plastic strain.[60] This particular conductor contains 25% bronze, 64% copper, 2.4% tantalum and 8.6% niobium (prior to reaction heat treatment). The plastic strain data were obtained with the applied load removed after straining sequentially to points along the total strain curve. For each of the applied magnetic fields I_c changes reversibly with strain to point 3 ($\varepsilon \cong 0.6\%$), and after that it changes irreversibly. Some dependence on reaction heat-treatment time was noted. Strain values marking the loss of reversibility increase to higher values for much shorter heat-treatment times, e.g., for 1-h heat treatment the points corresponding to 3 and 5 in Fig. 19 move to 1.1 and 0.7%, respectively. The onset of irreversible I_c-strain behavior is associated with crack formation in the Nb_3Sn compound.[61] Therefore such behavior marks the upper limit of a practical strain range.

The room-temperature strain tolerances of Nb_3Sn conductors are as stringent as their liquid-helium counterparts. Low-temperature strain tolerances are generally considered to be the worst case, however, and can be used as an indication of strains not to be exceeded during magnet construction.

A limited number of bend tests have been done for comparison with tensile-test data. Actual bending is done at room temperature. There is some evidence that bend strain tolerances are more stringent than tensile strain tolerances.[62,63]

More work is required however, particularly on the commercially available conductors, before a definite statement can be made.

The effects of irradiation on strain tolerances have only recently begun to receive attention. Variation of the strain dependence of the superconducting transition temperature, T_c, was studied in a Nb_3Sn conductor as a function of radiation-produced disorder.[64] From this study, T_c is plotted as function of reactor-spectrum-neutron fluence and presented in Fig. 20. By etching off the outer bronze matrix the residual compressive strain can be removed from the Nb_3Sn filament and a nearly strain-free state obtained. Comparing T_c values for these sample conditions yields a measure of the strain's influence on T_c.[65] Strain-induced T_c changes occur in conjunction with similar changes in I_c[66-68] and therefore extrapolation to critical-current behavior is possible. Fluences beyond 10^{18} decrease T_c and I_c should decrease accordingly. A 10% decrease in T_c results in approximately a 40% decrease in I_c.[19] The influence of residual compressive strain on T_c increases as the fluence exceeds 10^{18} suggesting that the critical current of neutron damaged material is somewhat more strain sensitive, ~7% is indicated in Fig. 18 for T_c. A neutron-damaged conductor should, therefore, exhibit a 28% higher value of I_c/I_{co} at the maximum in an I_c-strain curve. This increasing sensitivity to strain at the higher fluences is hown graphically in Fig. 21.

IV. Summary

A. NbTi

In present-day commercial-grade NbTi, neutron irradiation to the 10^{20} n/cm^2 fluence level decreases T_c only a few tenths of a degree. Decreases in I_c with increasing fluence are seen up to a level of ~20% degradation at which point no further decreases are seen (for room-temperature irradiations). Saturation of I_c degradations has not been observed for irradiations at low

temperature owing to the times necessary to accumulate the required fluences. The I_c degradiations are attributed to the reduction of the cell-wall pinning strength due to the increase of the normal-state resistivity of the cell interior. For irradiations at liquid-helium temperatures, 50 - 70% of this damage is recoverable by annealing the NbTi specimens to room temperature. In NbTi conductors I_c is relatively insensitive to the effects of str in. Most conductors can be strained as much as 4 - 5% without producing i versible degradiations. These strains approach the ultimate tensile stre th of the conductor and usually result in no more than ~30% reduction in I_c.

B. Nb_3Sn

The response of the critical properties of Nb_3Sn to neutron irradiation can be classified into the behavior at low fluences ($\lesssim 10^{18}$ n/cm^2) and at higher fluences. In the low-fluence regime ΔT_c changes are small and the dominant feature is an increase in the upper critical field which causes an increase in I_c. This increase is very field dependent, the higher relative increases increasing with applied field. For fields below ~3 T, monotonic decreases of I_c result as a function of fluence. These are attributed to normal-state-resistivity effects similar to those responsible for the I_c degradation in NbTi. For fluences above $>10^{18}$ n/cm^2 T_c monotonically decreases with fluence to a final value of 3.5 K reducing I_c and H_{c2} to zero (as measured at 4.2 K). The mechanism invoked for this T_c degradation involves the reduction of the electronic density of states owing to the increase of antisite disorder of the ordered compound. The response of the critical properties to high-energy neutrons is different in detail from that due to fission-reactor neutrons. Annealing to room temperature of damage incurred at low temperatures results in some recovery of T_c decreases, but would also result in recovery of H_{c2} increases. Adequate shielding of Nb_3Sn magnets is required for the <u>whole</u> magnet in order not to have "hot spots" which will result in degraded operation of the entire magnet system.

Strain effects in Nb_3Sn conductors are more severe than for NbTi conductors. The upper limit to a usable strain tolerance for the former is only of the order of 1 to 1.5%. This holds true for both room and cryogenic temperatures. Moreover, the superconducting critical properties of Nb_3Sn conductors exhibit appreciable variation within this strain range and such variations must be taken into account by magnet designers. Althrough experience is limited, it appears that Nb_3Sn multifilamentary conductors can, when appropriate care is taken, be employed successfully in the construction of a wide variety of magnets.

References

1. For a recent review of radiation effects in superconductors see A. R. Sweedler, C. L. Snead, Jr., and D. E. Cox, Treatise on Materials Science and Technology, New York, NY, 1979, Academic Press, 14, pps. 349-426.

2. S. Klaumünzer, G. Ishenko, and P. Müller, *Z. Phys.* 268, (1974) 189.

3. H. Ullmaier, C. Papastaikoudis, and W. Schilling, *Phys. Status Solidi* 38, (1970) 189.

4. H. Ullmaier, K. Papastaikaudis, S. Takács, and W. Schilling, *Phys. Status Solidi* 41, (1970) 671.

5. M. Söll, C. A. M. van der Klein, H. Bauer, and G. Vögel, *IEEE Trans. on Magn.* MAG-11, (1975). 178.

6. M. Söll, PhD. thesis Technische Universität München (September 1974) (unpublished).

7. A. V. Narlikar and D. Dew-Hughes, *J. Mater. Sci.* 1, (1966) 317.

8. D. F. Neal, A. C. Barber, A. Woolcock, and J. A. F. Gidley, *Acta Metall.* 19, (1971) 143.

9. R. G. Hampshire and M. T. Taylor, *J. Phys. F.* 2, (1972) 89.

10. M. Söll, S. L. Wipf, and G. Vögl, Proc. Appl. Supercond. Conf. IEEE Publ. No. 72 CH0682-5-TABSC, (1972) 434.

11. D. Dew-Hughes and M. J. Witcomb, *Philos. Mag.* 26, (1972) 73.

12. B. S. Brown, T. H. Blewitt, T. L. Scott, and A. C. Klank, *J. Nucl. Mater.* 52, (1974) 215.

13. C. L. Snead, Jr., L. Nicolosi, and W. Tremel, *Appl. Phys. Lett.* 31, (1977) 31.

14. D. M. Parkin and A. R. Sweedler, *IEEE Trans. Magn.* MAG-11 (1975) 166.

15. See for instance D. M. Parkin and C. L. Snead, Jr., Proc. Int. Conf. Fundamental Aspects Radiat. Damage Met. (M. T. Robinson and F. W. Young, Jr., eds.), CONF-751006 (1975) 1162.

16. S. T. Sikula, *J. Nucl. Mat.* 72, (1978) 91.

17. M. Couach, J. Doulat, and E. Bonjour, *IEEE Trans. Magn.* MAG-11, (1975) 170.

18. D. S. Easton and C. C. Koch, *Advances in Cryogenic Engrg.* 22, (1977) pps. 453-462.

19. D. S. Easton, D. M. Kroeger, and A. Moazed, *Appl. Phys. Letts.* 29, (1976) pps. 382-384.

20. C. C. Koch and D. S. Easton, *Cryogenics* 17, (1977) 391.

21. D. S. Easton and C. C. Koch, Shape Memory Effects in Alloys, ed. by J. Perkins.

22. J. W. Ekin, *IEEE Trans. Magn.* MAG-13, (1977) 127.

23. E. S. Fisher and S. H. Kin, ibid., 112.

24. J. W. Ekin, F. R. Ficket, and A. F. Clark, *Adv. Cryog. Eng.* 22, (1977) 449.

25. R. P. Reed, R. P. Mikesel, and A. F. Clark, ibid., 463.

26. W. C. Young and R. W. Boom Proc. 4th Conf. on Magnet Technology, Brookhaven National Laboratory, USAEC CONF-720908, ed. by Y. Winterbotton (1972) 224.

27. M. Suenaga, private communication.

28. E. S. Fisher and S. H. Kim, *IEEE Trans. Magn.* MAG-13, (1977) 112.

29. For a review of the metallurgy of NbTi and Nb_3Sn conductors see Treatise on Materials Science and Technology, New York, NY 1979, Academic Press, eds. Thomas Luhman and David Dew-Hughes.

30. A. D. McInturff, private communication.

31. R. Bett, *Cryogenics* 14, (1974) 361.

32. A. R. Sweedler, et al., Int. Conf. Radiat. Effects Tritium Technol. Fusion Reactors, Gatlinburg, Tennessee, CONF-750989, Vol. II, (1976) 442.

33. A. R. Sweedler, D. G. Schweitzer, and G. W. Webb, *Phys. Rev. Letts.* 33, (1974) 168.

34. A. R. Sweedler, D. E. Cox, and L. Newkirk, *J. Electron Mater.* 4, (1975) 883.

35. A. R. Sweedler, D. E. Cox, and S. Moehlecke, *J. Nucl. Mater.* 72, (1978) 50.

36. A. R. Sweedler, D. Cox, D. G. Schweitzer, and G. W. Webb, *IEEE Trans. Magn.* MAG-11 (1975) 163.

37. S. Moehlecke, Ph.D. thesis, Univ. of Campinas, Brazil (1977) (unpublished).

38. T. L. Francavilla, B. N. Das, D. U. Gubser, R. S. Meussner, and S. T. Sekula, *J. Nucl. Mater.* 72, (1978) 203.

39. T. L. Francavilla, R. A. Meussner, and S. T. Sekula, *Solid State Commun.* 23 (1977) 207.

40. A. I. Skvortsov, Y. V. Shemeljov, V. E. Klepatski, and B. M. Levitski, *J. Nucl. Mater.* 72, (1978) 198.

41. A. R. Sweedler and D. E. Cox, *Phys. Rev.* 12, (1975) 147.

42. A. E. Karkin, V. E. Arkhipov, B. N. Goshchitskii, E. P. Romanov, and S. K. Sidorov, *Phys. Status Solidi (a)* 38, (1976) 433.

43. B. S. Brown, R. C. Birtcher, R. T. Kampwirth, and T. H. Blewitt, *J. Nucl. Mat.* 72, (1978) 76.

44. D. O. Welch, G. J. Dienes, and R. D. Hatcher, *Bull. Am. Phys. Soc.* 25, (1980) 331.

45. D. G. Schweitzer and D. M. Parkin, *Appl. Phys. Lett.* 24, (1974) 333.

46. D. M. Parkin and D. G. Schweitzer, *Nucl. Technol.* 22, (1974) 108.

47. B. S. Brown, T. H. Blewitt, D. G. Wozniak, and M. Suenaga, *J. Appl. Phys.* 46, (1975) 5163 and B. S. Brown, T. H. Blewitt, T. L. Scott, and D. G. Wozniak, *J. Appl. Phys.* 49, (1978) 4144.

48. C. L. Snead, Jr. and D. M. Parkin, *Nucl. Technol.* 29, (1976) 264.

49. Edward J. Kramer, *J. Appl. Phys.* 44, (1973) 1360.

50. For the most recent review of flux-pinning effects in irradiated material see Edward J. Kramer, *J. Nucl. Mater.* 72, (1978) 5.

51. M. Söll, H. Bauer, K. Böning, and R. Bett, *Phys. Lett.* 51A, (1975) 83.

52. C. L. Snead, Jr., *J. Nucl. Mater.* 72, (1978) 192.

53. C. L. Snead, Jr., Don M. Parkin, M. W. Guinan, and R. A. Von Konynenburg, Proc. of the Second Topical Meeting on the Techn. of Controlled Nuclear Fusion, Vol. I, G. L. Kulciusky, ed., CONF-760935-P1, (1976) pps 229-237.

54. R. M. Scanlan and E. L. Raymond, *IEEE Trans. Magn.* MAG-15, (1979) 56.

55. C. F. Old and J. P. Charlesworth, *Cryogenics,* (August 1976) 469.

56. I. L. McDougall, *IEEE Trans. Magn.* MAG-11, (1975) 1467.

57. G. Rupp, *IEEE Trans. Magn.* MAG-15, (1979) 109.

58. G. Rupp, *Cryogenics,* (December 1978) 663.

59. T. S. Luhman and D. O. Welch, Topical Conference on Filamentary A15 Superconductors, May 28-29, 1980, Brookhaven National Laboratory, Upton, NY.

60. W. Specking, D. E. Easton, D. M. Kroger, and P. A. Sanger, *Adv. in Cryogenic Eng.* 26, (1980).

61. Thomas Luhman, M. Suenaga, D. O. Welch, and K. Kaiho, *IEEE Trans. Magn.* MAG-15, (1979) 699.

62. Thomas Luhman and D. O. Welch, to be published in Proc. of the 8th Symp. on Eng. Problems of Fusion Research, San Francisco, CA, November 13-16, 1979.

63. K. Kaiho, T. Luhman, M. Suenaga, and W. B. Sampson, to be published in *Appl. Phys. Letts.* 1980.

64. Data courtesy of C. L. Snead, Jr., Brookhaven National Laboratory, published by D. O. Welch in proceedings of Cryogenic Eng. Conf./Int. Cryogenic Materials Conf. 1979, Advances in Cryogenic Eng., Vol. 26, 1980.

65. Thomas Luhman and M. Suenaga, *IEEE Trans. Magn.* MAG-13, (1977) 800.

66. Thomas Luhman and M. Suenaga, *Applied Phys. Letts.* 29, (1976) 61.

67. T. Luhman, M. Suenaga, and C. J. Klamut, *Advances in Cryogenic Engineering* 24, (1978) 325.

68. C. L. Snead, Jr., unpublished work.

Figure Captions

Figure 1. Critical-current density as a function of applied field for NbTi irradiated at 5 K to a fluence of 3.2 10^{18} n/cm^2 (b) and 7.5 x 10^{18} n/cm^2 (c) (E > 0.1 MeV). Curves d and e denote anneals to 100 and 270 K, respectively. After Söll et al., ref. 10.

Figure 2. Schematic of the decrease of $\Delta\kappa$ pinning of dislocation cell walls in NbTi owing to the increase in the κ of the cell interior relative to that of the walls. After Dew-Hughes and Witcomb, ref. 11.

Figure 3. Ambient fission-reactor irradiation (open circles) and 4.2 K 30-GeV-proton irradiation (solid curcles). The latter is plotted as a function of "equivalent neutrons" based upon damage-energy comparisons. After Snead et al., ref. 13.

Figure 4. The effect of temperature on the ultimate tensile strength and percent strain of a Cu/NbTi composite. Sample size 1.44 x 2.90 mm, Cu-Ni:Cu:NbTi 0:2.8:1, Ti volume percentage 26, number of filaments 18, filament diameter 279.4 μm, untwisted. After D. S. Easton and C. C. Koch, ref. 18.

Figure 5. Critical current as a function of applied tensile strain for a Nb-34 Ti and a Nb_3Sn conductor. Specifications of the NbTi conductor are, sample size of 0.58 x 0.68 mm, NbTi:Cu 1:1.8, 180 filaments, 0.8 turns per cm, tests made of 5 tesla; for the Nb_3Sn conductor sample size 0.33 x 0.66 mm, 3553 Nb filaments, filament diameter 3.6 μm, 11 cm twist length, reinforced Nb_3Sn 7 strand, 0.15 mm strand diameter, 6 x 240 Nb filaments, filament diameter 6 μm, 1.3 cm filament twist, 0.18 cm cable twist, center filament 304 s.s. tests made at 9 tesla. After J. W. Ekin, ref. 22.

Figure 6. Reduced T_c vs. fission-reactor neutron fluence for several A15 compounds. After Sweedler et al., ref. 34.

Figure 7. T_c and ρ_N as a function of fluence for neutron irradiation at 20 K. After Brown et al., ref. 43.

Figure 8. Isochronal recovery of T_c and ρ_N following 20-K neutron irradiation. Upturn of $\Delta\rho$ at ~500 K is considered an antifact. After Brown et al., ref. 43.

Figure 9. The reduced critical-current density of filamentary Nb_3Sn is plotted as a function of neutron fluence at helium temperatures with the measuring field parametrized. Also shown is the recovery behavior upon annealing to nitrogen and room temperature. After Brown et al., ref. 47.

Figure 10. The critical current of neutron-irradiated (~150°C) Nb_3Sn filamentary wires is plotted as a function of applied magnetic field for a range of fluences. After Snead and Parkin, ref. 48.

Figure 11. The reduced critical current of neutron-irradiated Nb_3Sn filamentary wires is plotted as a function of fluence with the measuring field parametrized. The increase of I_c with fluence at low fluences, with greater increases at the higher fields is noted. The field independence of the I_c reduction at high fluences is evidenced by the uniform response after ~2 x 10^{18} n/cm^2. After Snead and Parkin, ref. 48.

Figure 12. The critical current of Nb_3Sn is plotted as a function of applied field. The results for two fluence segments are shown with an anneal to 273 K shown after the low-fluence segment. After Snead, ref. 52.

Figure 13. A comparison between the critical-current degradation of NbTi and Nb_3Sn for identical 30-GeV-proton irradiations and anneals. The critical-currents were determined at 4 T. Anneals are for 273 K for the low-fluence point, and for 77 and 273 K for the high-fluence data. After Snead, ref. 52.

Figure 14. The normal-to-superconducting transition for a Nb_3Sn single-core specimen is plotted for a 30-GeV-proton fluence of 1.6×10^{18} /cn^2 at 4.2 K. The upper dashed curve shows the transition prior to the irradiation. The lower-temperature dashed curve is one obtained for a neutron-irradiated identical specimen to a fluence that produced the same I_c reduction as measured for the proton-irradiated specimen. After Snead, ref. 52.

Figure 15. The critical current vs. applied field is plotted as a function of low-fluence 14-MeV-neutron irradiations at room temperature. Note only decreases are seen for fields below ~30 hb, with an apparent crossover at that point. After Snead et al., ref. 53.

Figure 16. The critical current is plotted vs. applied field for two fluences of 14-MeV-neutron irradiations performed at room temperature. Also plotted for comparison are the result for two comparable fluences of fission-reactor neutrons. After Snead et al., ref. 53.

Figure 17. Typical load-strain curves for Nb_3Sn multifilamentary conductors. A-conductor with less than 16% niobium prior to reaction, B-conductor with more than 16% niobium prior to reaction. After C. F. Old and J. P. Charlesworth, ref. 55.

Figure 18. Critical current I_c relative to I_{co} (for zero stress) as a function of strain ε of differently heat treated multifilamentary Nb_3Sn conductors and a NbTi multifilamentary conductor (curve 7) 4.2 K and 4.4 T after G. Rupp, ref. 58.

Figure 19. Critical current as a function of total and plastic strain at 3, 5, and 7 T and 4.2 K for a 30 hour heat treatment at 700°C. Conductor specifications following the reaction heat treatment. Volume percent niobium 0.5, percent Nb_3Sn 10.7, percent niobium converted to Nb_3Sn 94.6, 1.72 μm layer thickness and 0.7 wt percent Sn re-

maining in bronze. After W. Specking, D. S. Easton, D. M. Kroeger, and P. A. Sanger, ref. 60.

Figure 20. The superconducting transition temperature (inductive mid-point) as a function of reactor spectrum neutrons for a single core Nb_3Sn conductor whose bronze to niobium ratio is 15:1. Reaction heat treatment time was 4 d at 700°C to produce a 6-μm thick Nb_3Sn layer. After C. L. Snead, Jr., ref. 64 and 68.

Figure 21. The change in T_c [$(-\Delta T_c = T_c$ (bronze on) - T_c (bronze off)] for single-core Nb_3Sn specimens as a function of fission-reactor neutron fluence. The enhancement of the strain effect due to the bronze is evident in the increases after $\sim 10^{19}$ n/cm^2. After C. L. Snead, Jr., ref. 64 and 68.

Table 1

CHARACTERISTICS OF FILAMENTARY CONDUCTORS
(After G. Rupp, Ref. 57)

Filament	Dimension (mm)	α	Diffision	d (μm)	γ	I_{co} (4.4 T) (AMP)	No. Fig. 4
1615	0.65 x 0.25	4	700°C/64h	1.3	0.22	252	1
			/16h	1.0	0.18	210	2
			/ 4h	0.7	0.13	173	3
61	0.15 x 0.44	4	750°C/64h	4.8	0.24	36	4
			/14h	2.0	0.11	40	5
			650°C/24h	1.0	0.06	20	6
60 NbTi	ϕ 0.4					128	7

α: cross sectional area of bronze to that of Nb

d: layer thickness of Nb_3Sn

γ: cross sectional area of Nb_3Sn to that of bronze

I_{co}(4.4 T): critical current before straining at 4.4 Tesla

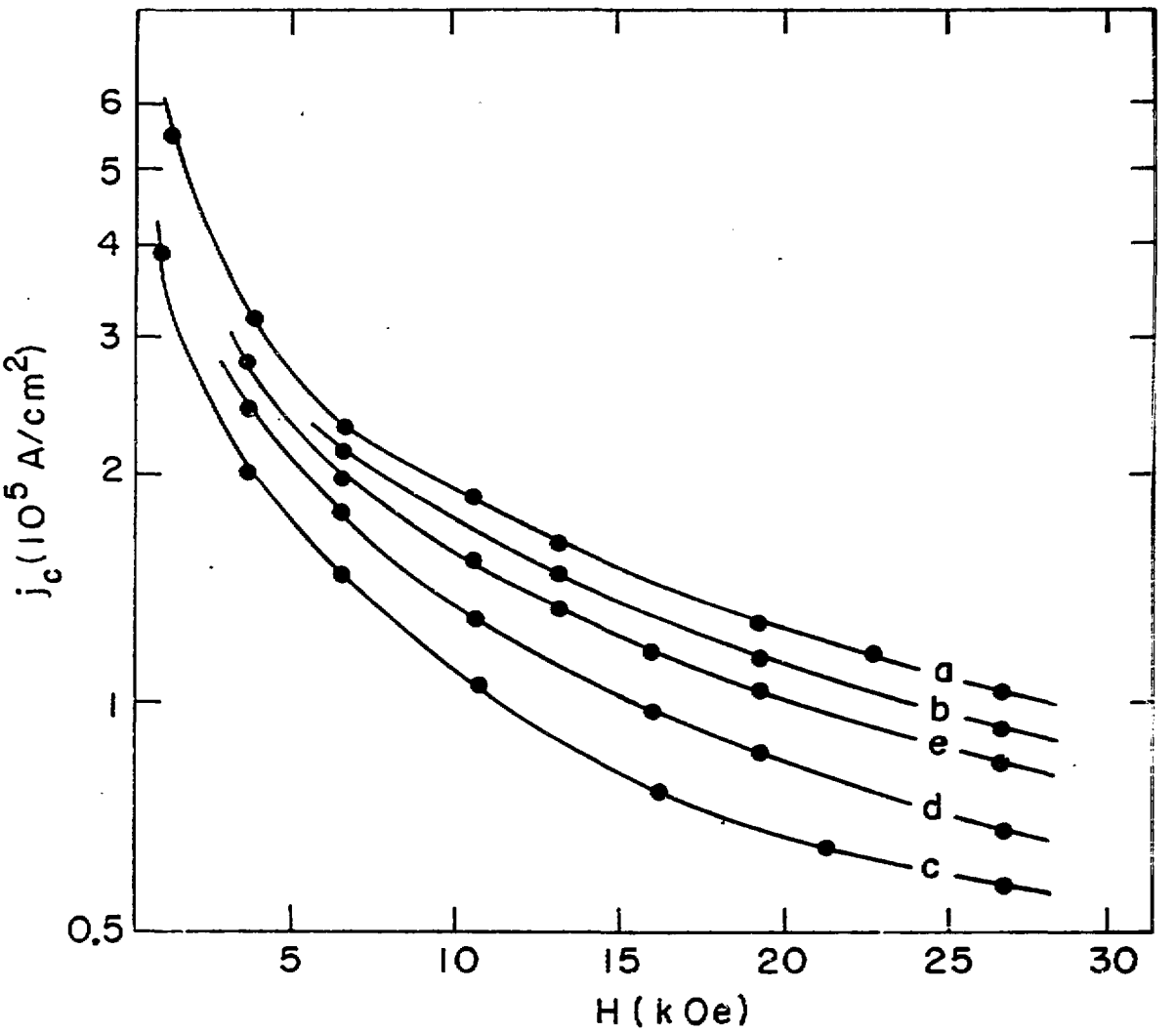

FIGURE 1.

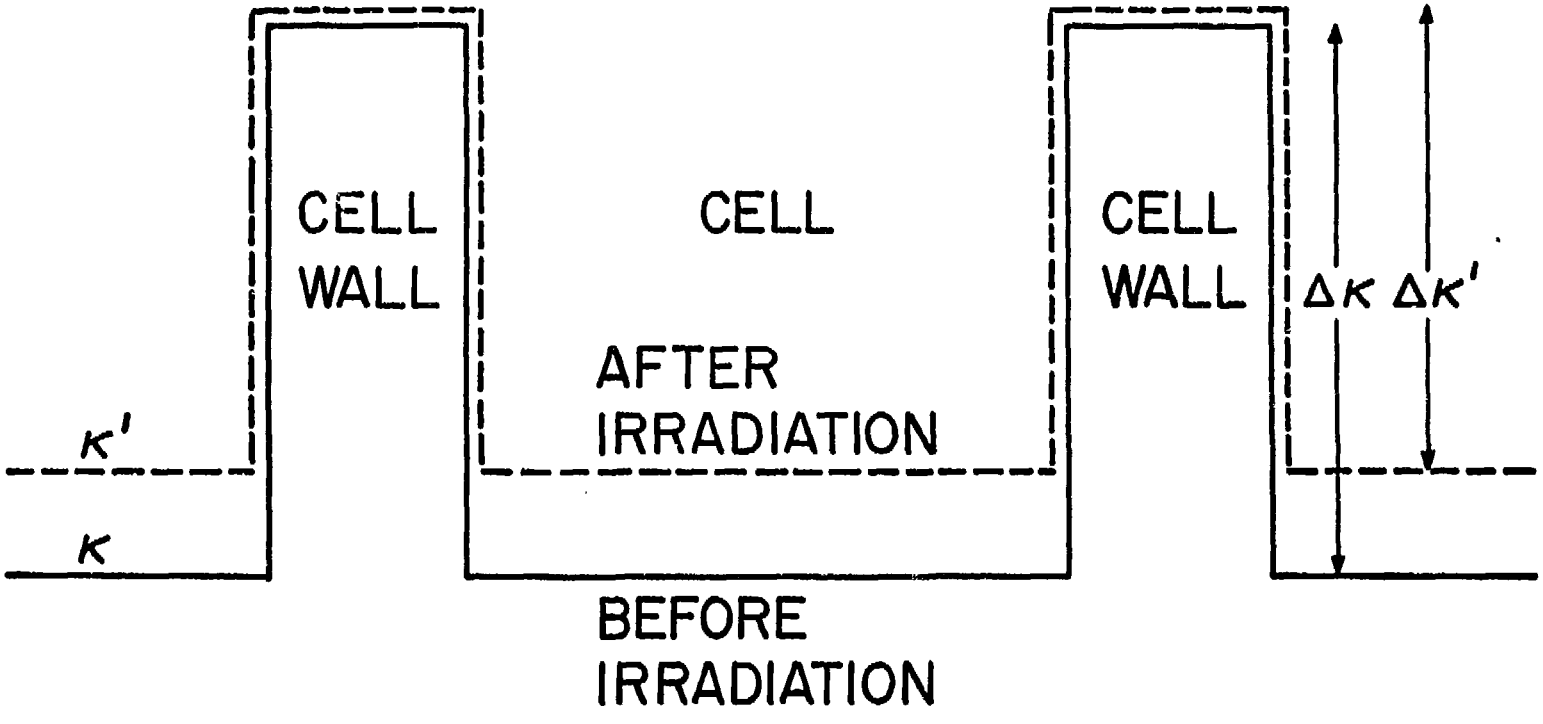
CELL WALL
CELL
CELL WALL
ΔK ΔK'
AFTER IRRADIATION
K'
K
BEFORE IRRADIATION

FIGURE 2.

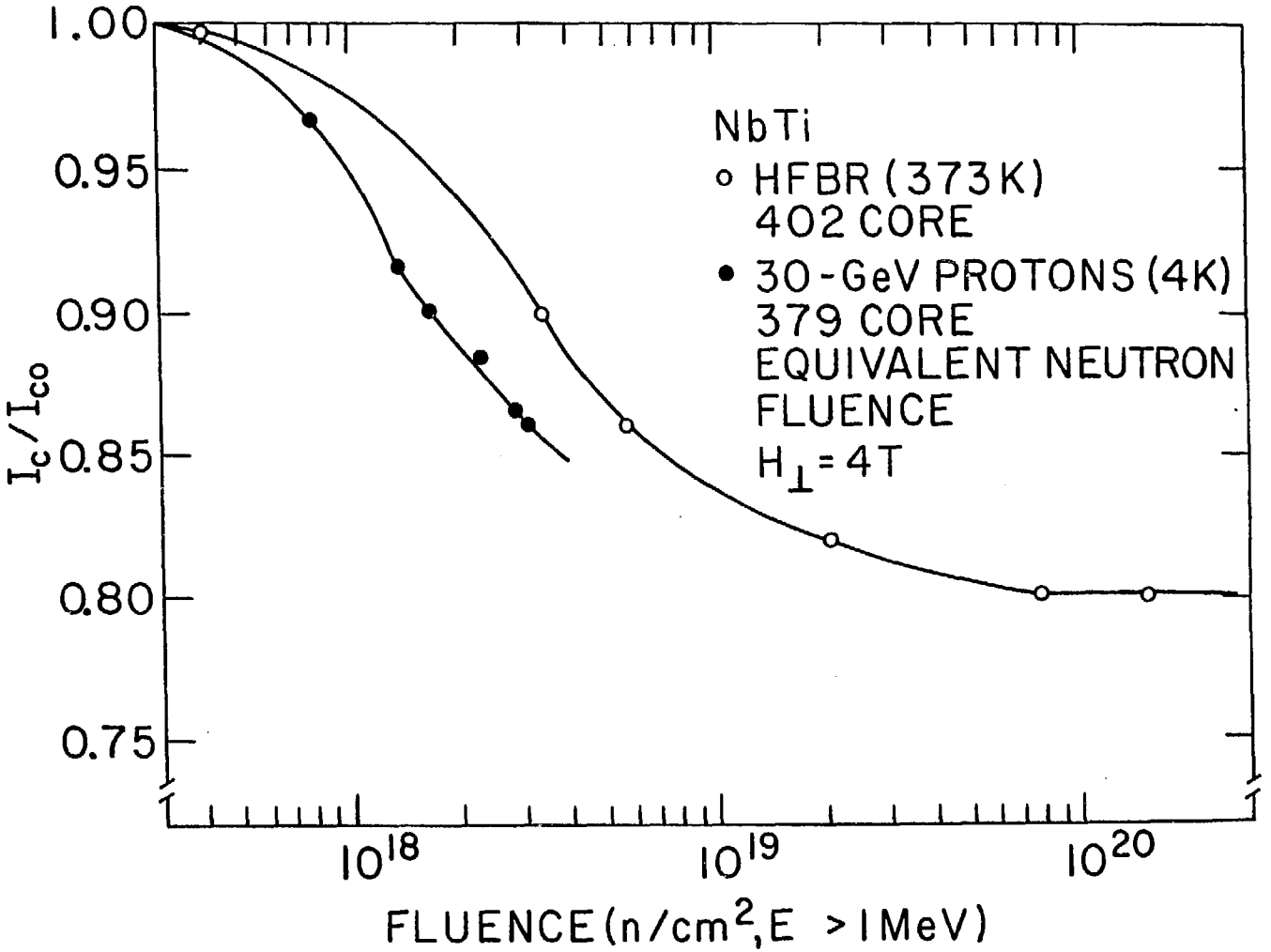
1.00
0.95
0.90
0.85
0.80
0.75
I_c/I_{co}
NbTi
○ HFBR (373K)
402 CORE
● 30-GeV PROTONS (4K)
379 CORE
EQUIVALENT NEUTRON
FLUENCE
$H_\perp = 4T$
10^{18}
10^{19}
10^{20}
FLUENCE ($n/cm^2, E > 1MeV$)

FIGURE 3.

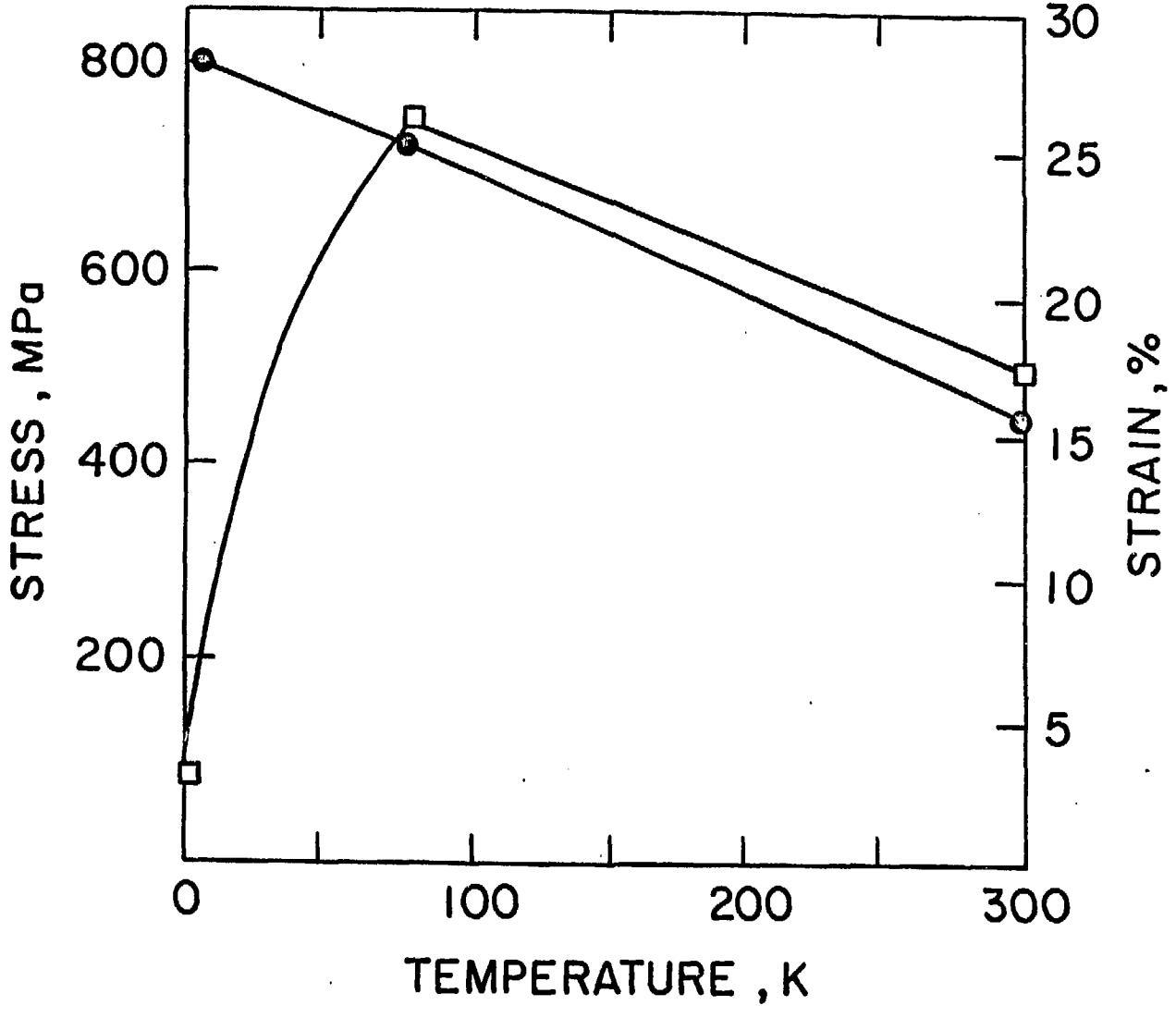
800
600
400
200
STRESS , MPa
30
25
20
15
10
5
STRAIN , %
0
100
200
300
TEMPERATURE , K

FIGURE 4.

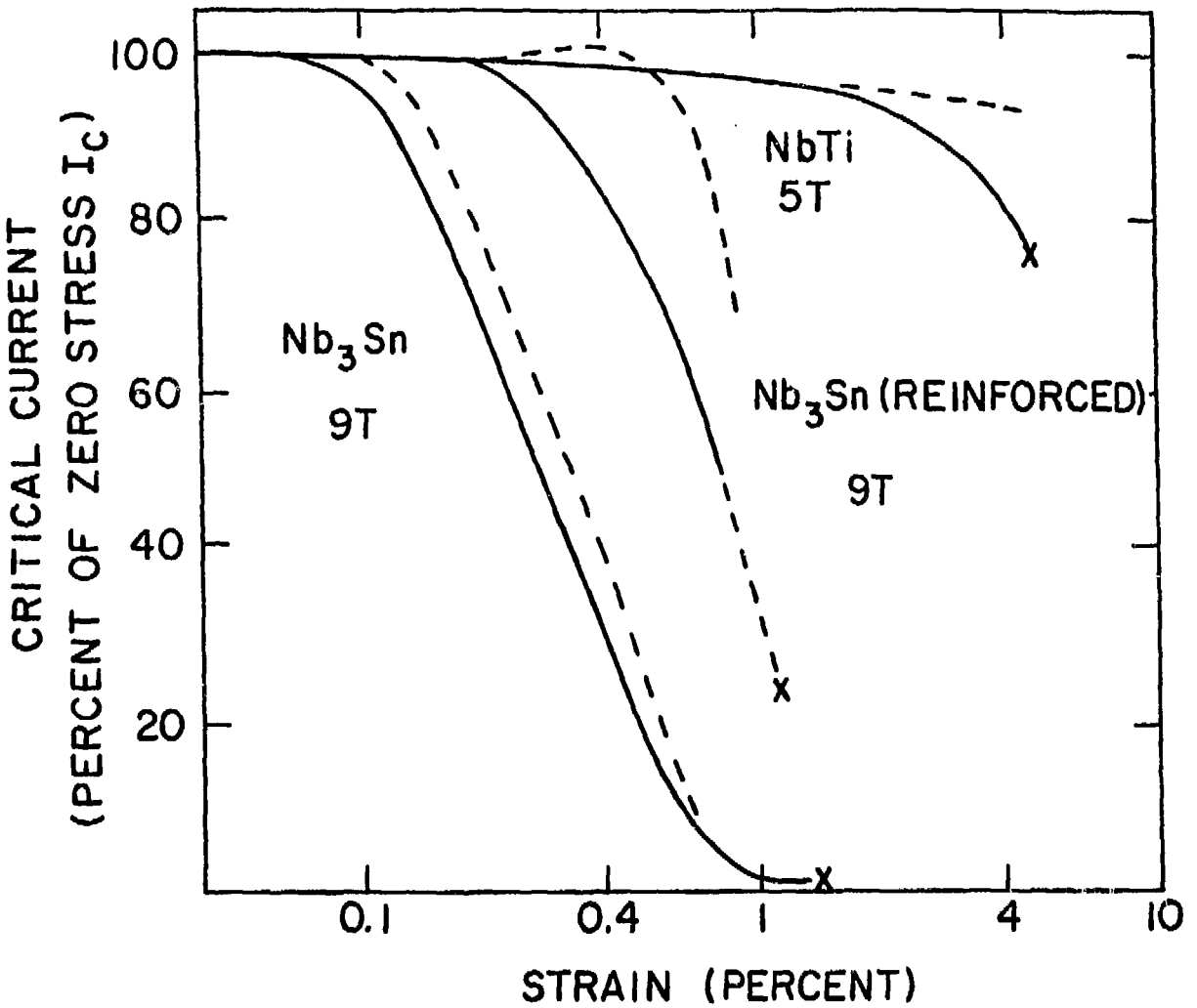
CRITICAL CURRENT
(PERCENT OF ZERO STRESS I_c)
100
80
60
40
20
0.1
0.4
1
4
10
STRAIN (PERCENT)
NbTi
5T
Nb_3Sn
9T
Nb_3Sn (REINFORCED)
9T

FIGURE 5.

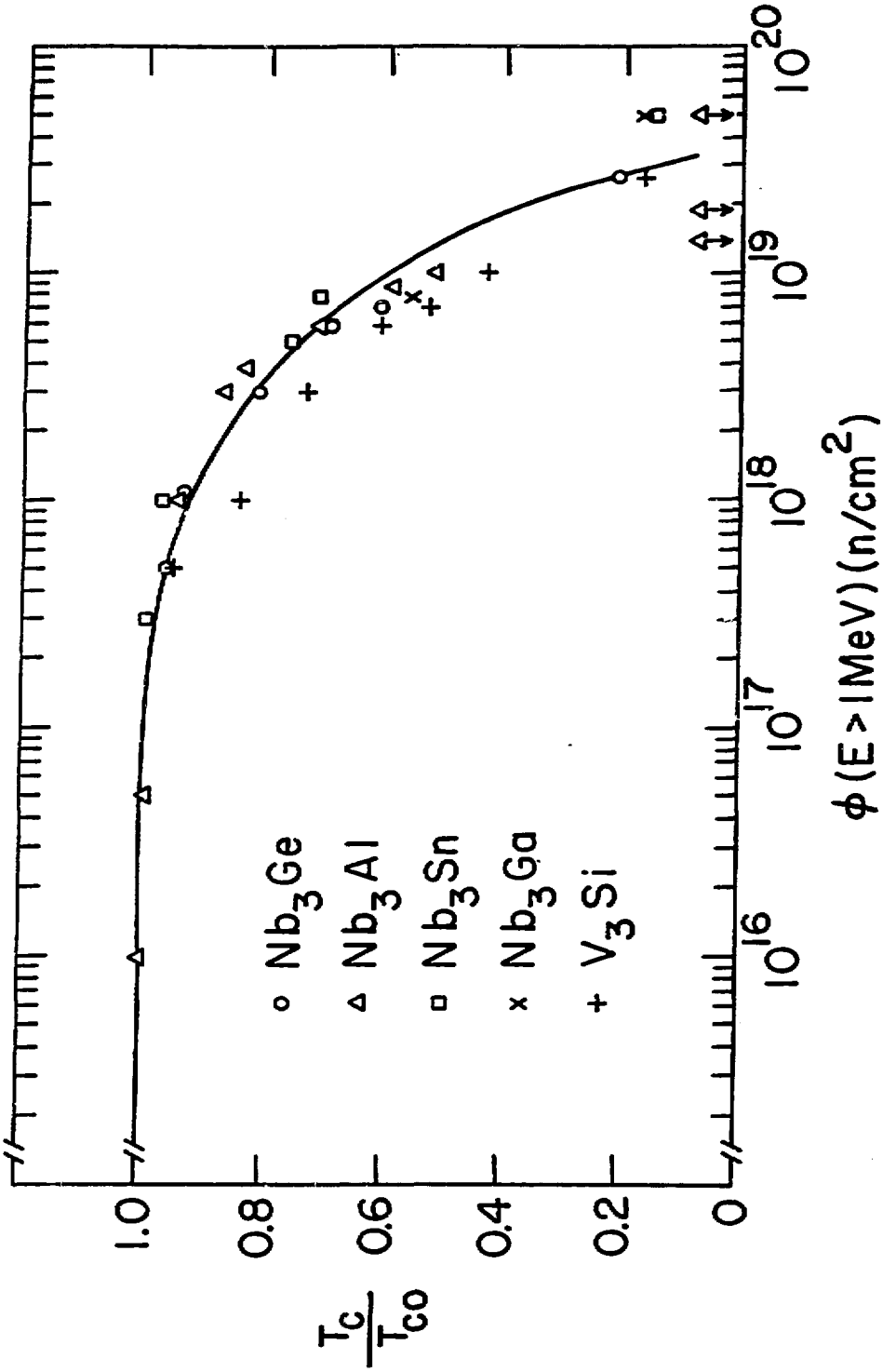
1.0
0.8
0.6
0.4
0.2
0
$\frac{T_c}{T_{co}}$
10^{16}
10^{17}
10^{18}
10^{19}
10^{20}
$\phi(E>1MeV)(n/cm^2)$
o Nb_3Ge
Δ Nb_3Al
□ Nb_3Sn
× Nb_3Ga
+ V_3Si

FIGURE 6.

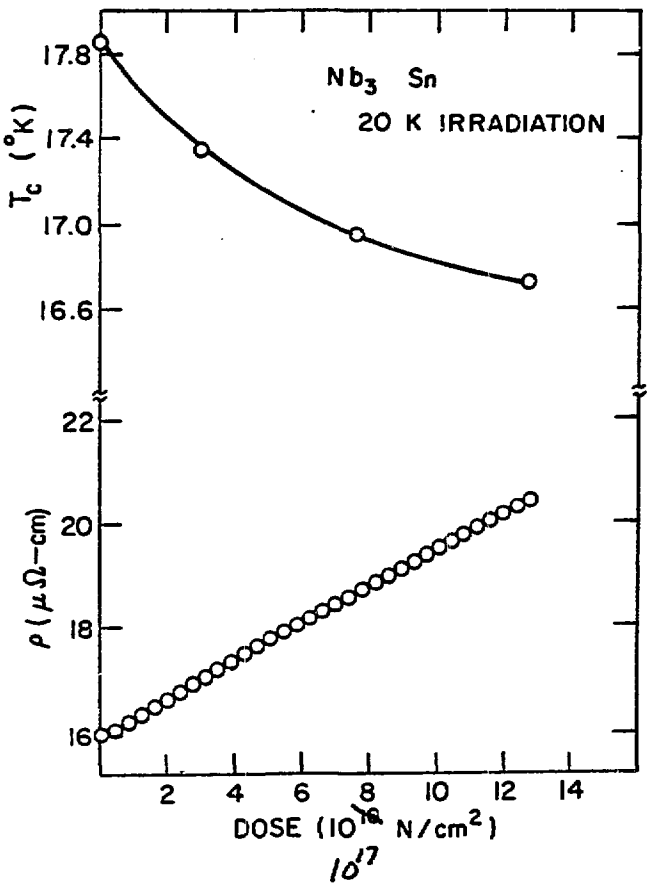

FIGURE 7.

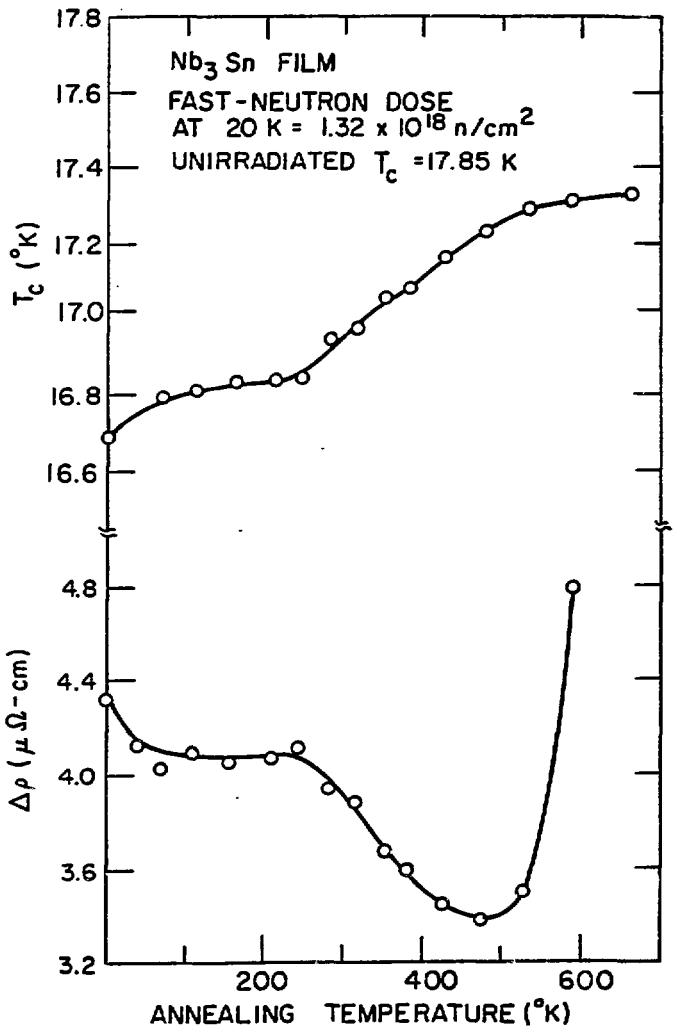

FIGURE 8.

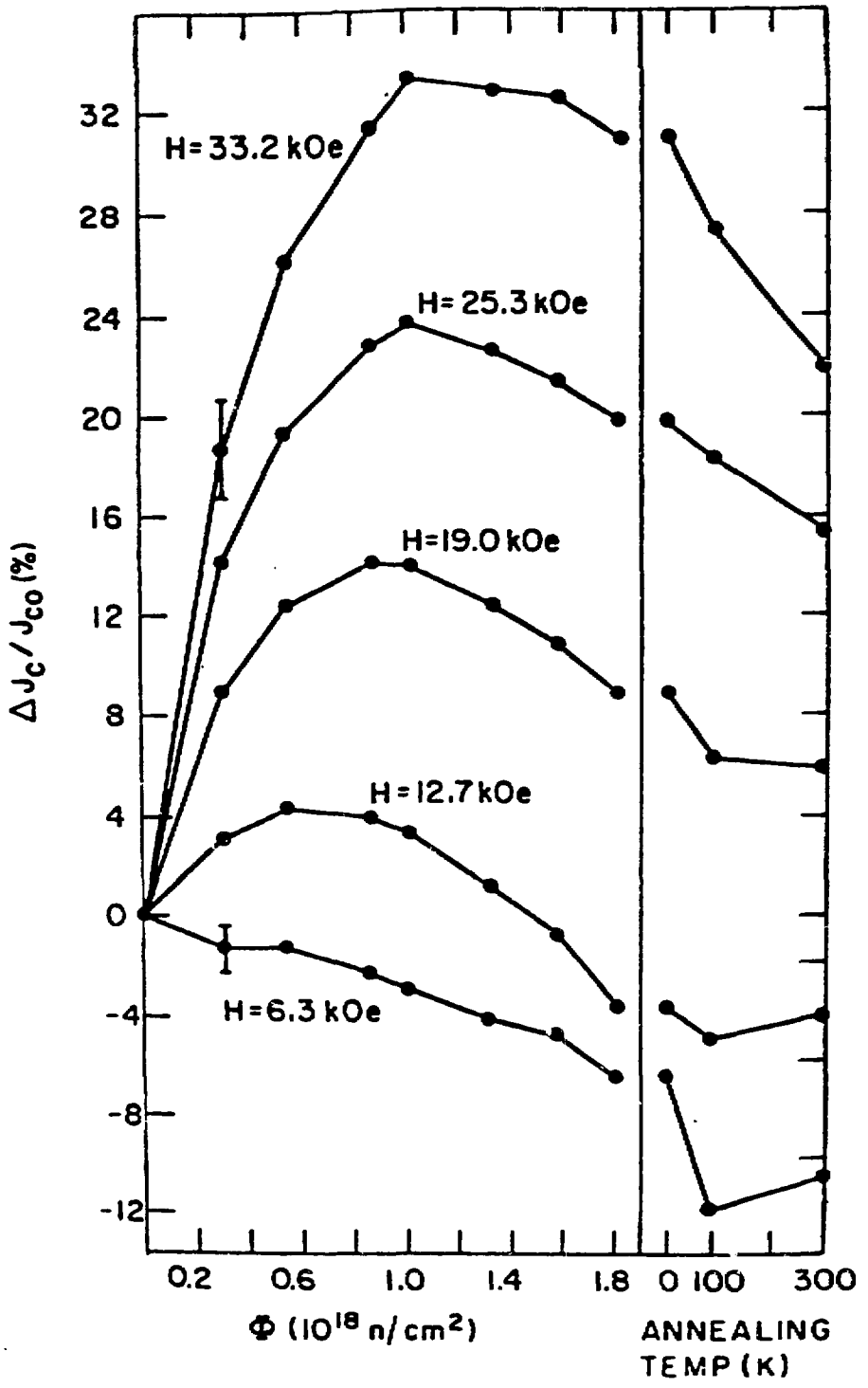
H=33.2 kOe
H=25.3 kOe
H=19.0 kOe
H=12.7 kOe
H=6.3 kOe
ΔJc / Jco (%)
32
28
24
20
16
12
8
4
0
-4
-8
-12
0.2
0.6
1.0
1.4
1.8
Φ (10^18 n/cm^2)
0
100
300
ANNEALING TEMP (K)

FIGURE 9.

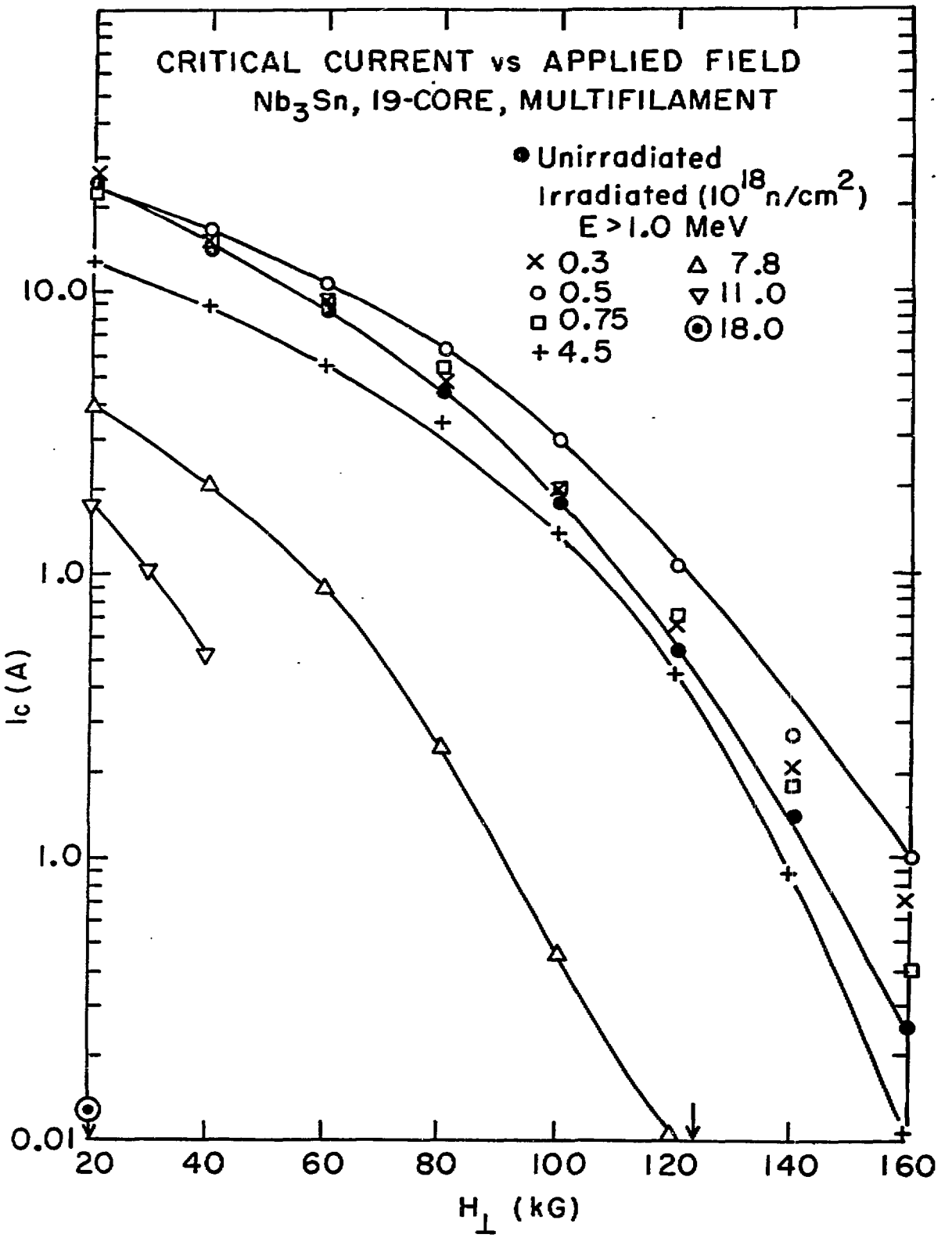
CRITICAL CURRENT vs APPLIED FIELD
Nb3Sn, 19-CORE, MULTIFILAMENT
Unirradiated
Irradiated (10^18 n/cm^2)
E > 1.0 MeV
× 0.3
○ 0.5
□ 0.75
+ 4.5
△ 7.8
▽ 11.0
⊙ 18.0
10.0
1.0
1.0
0.01
Ic (A)
20
40
60
80
100
120
140
160
H⊥ (kG)

FIGURE 10.

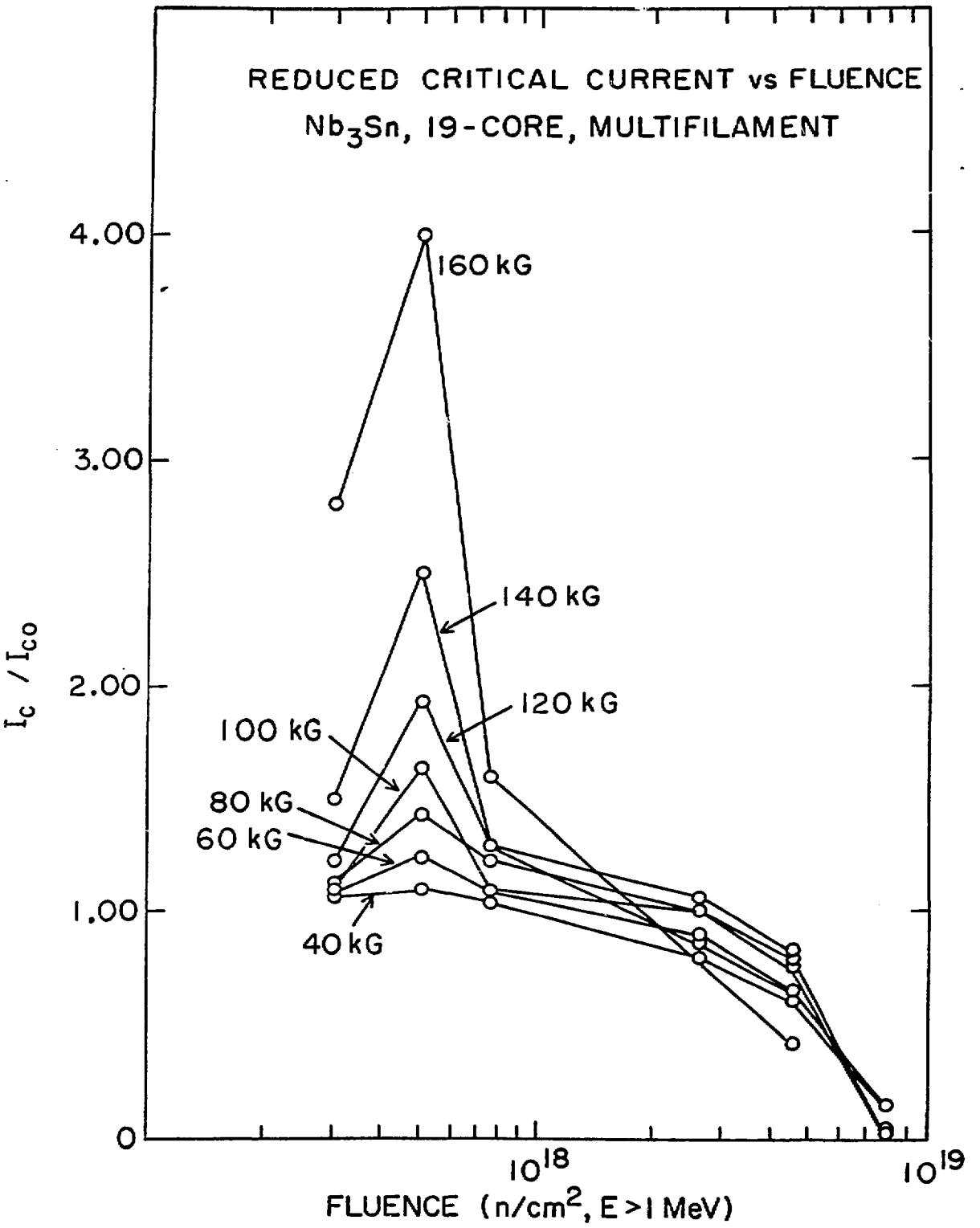
REDUCED CRITICAL CURRENT vs FLUENCE
Nb3Sn, 19-CORE, MULTIFILAMENT
4.00
3.00
2.00
1.00
0
Ic / Ico
160 kG
140 kG
120 kG
100 kG
80 kG
60 kG
40 kG
10^18
10^19
FLUENCE (n/cm^2, E>1 MeV)

FIGURE 11.

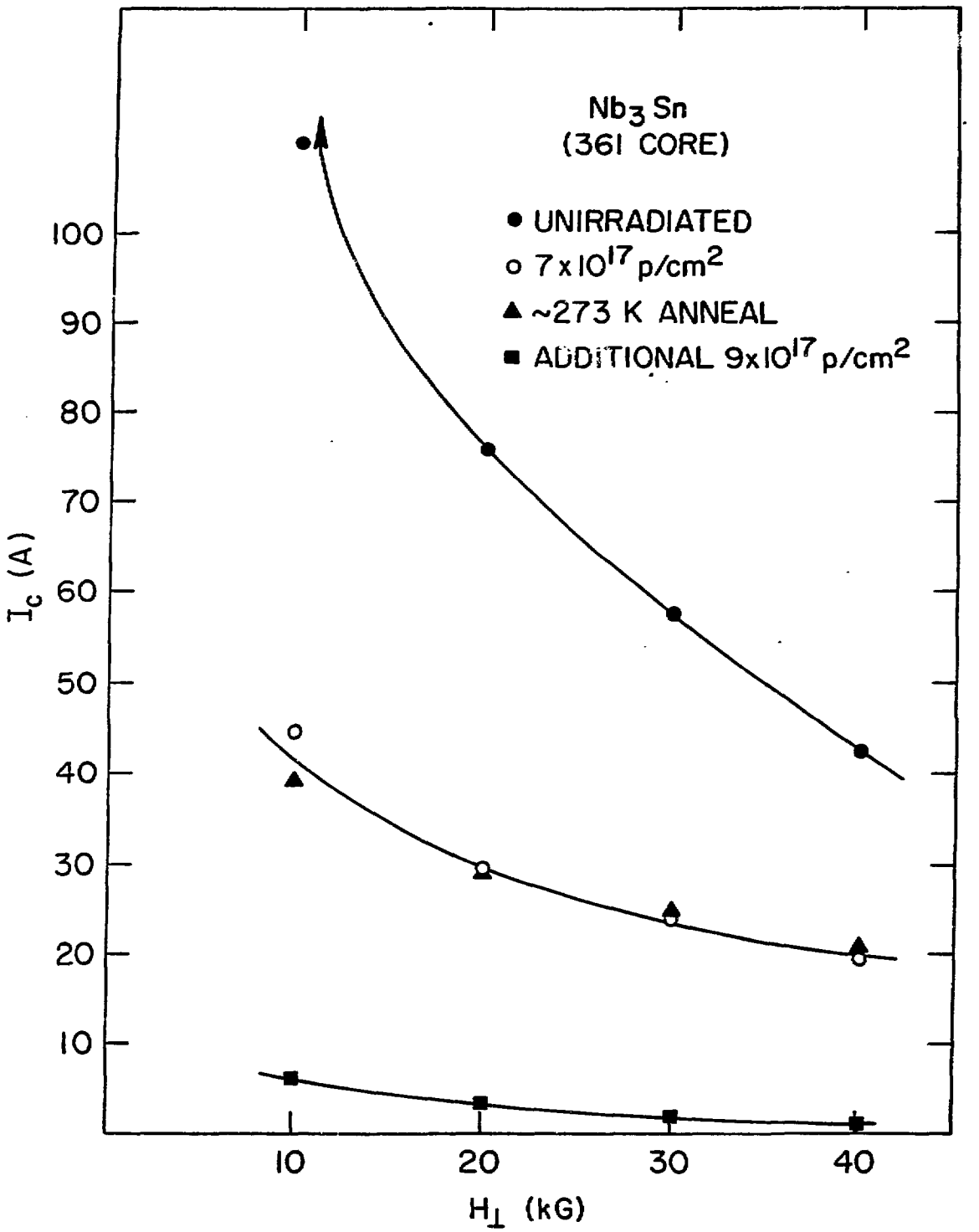
Nb3 Sn
(361 CORE)
● UNIRRADIATED
o 7x10^17 p/cm^2
▲ ~273 K ANNEAL
■ ADDITIONAL 9x10^17 p/cm^2
Ic (A)
100
90
80
70
60
50
40
30
20
10
10
20
30
40
H⊥ (kG)

FIGURE 12.

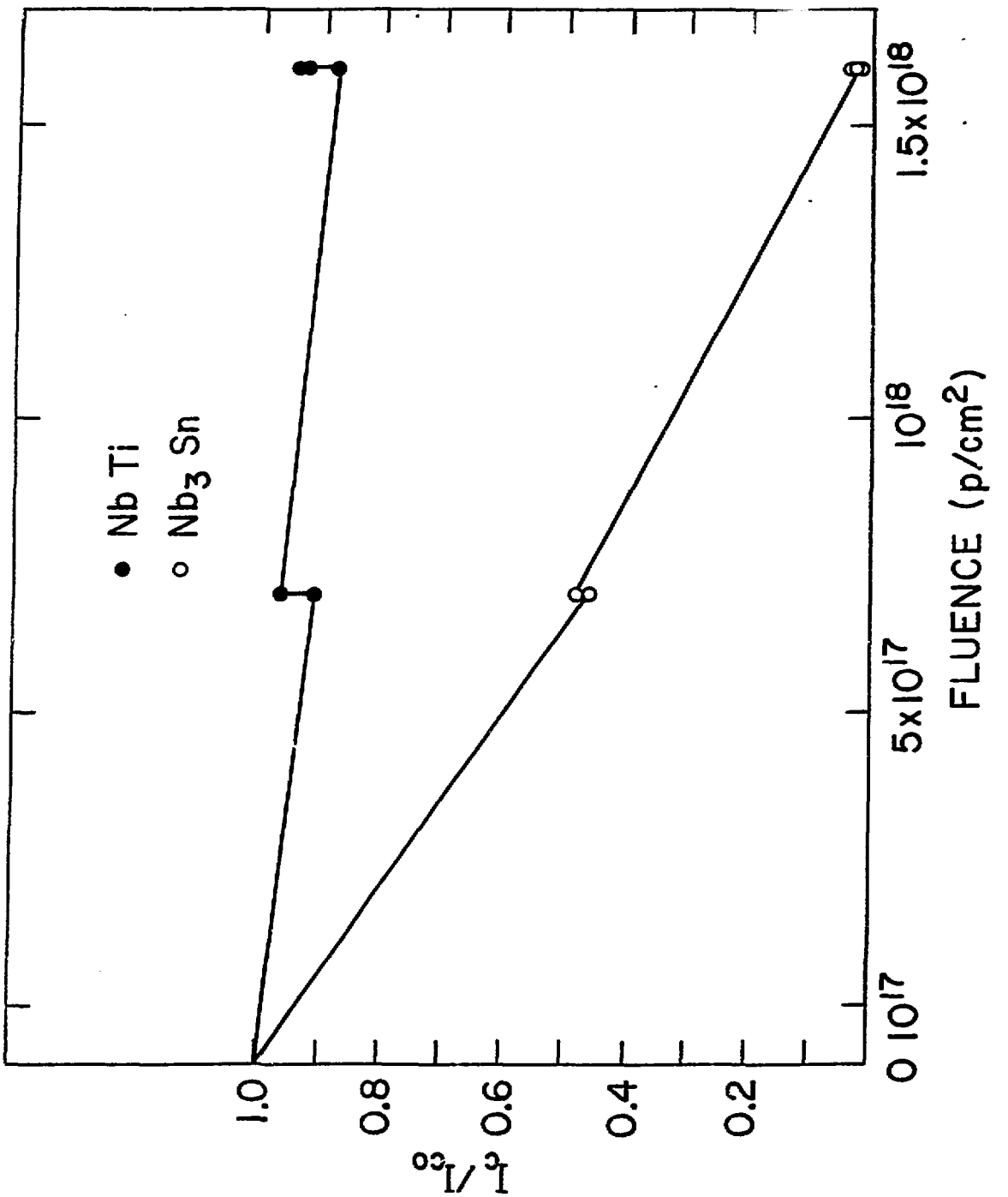
• Nb Ti
○ Nb_3 Sn
I_c/I_{co}
1.0
0.8
0.6
0.4
0.2
0
10^{17}
5×10^{17}
10^{18}
1.5×10^{18}
FLUENCE (p/cm^2)

FIGURE 13.

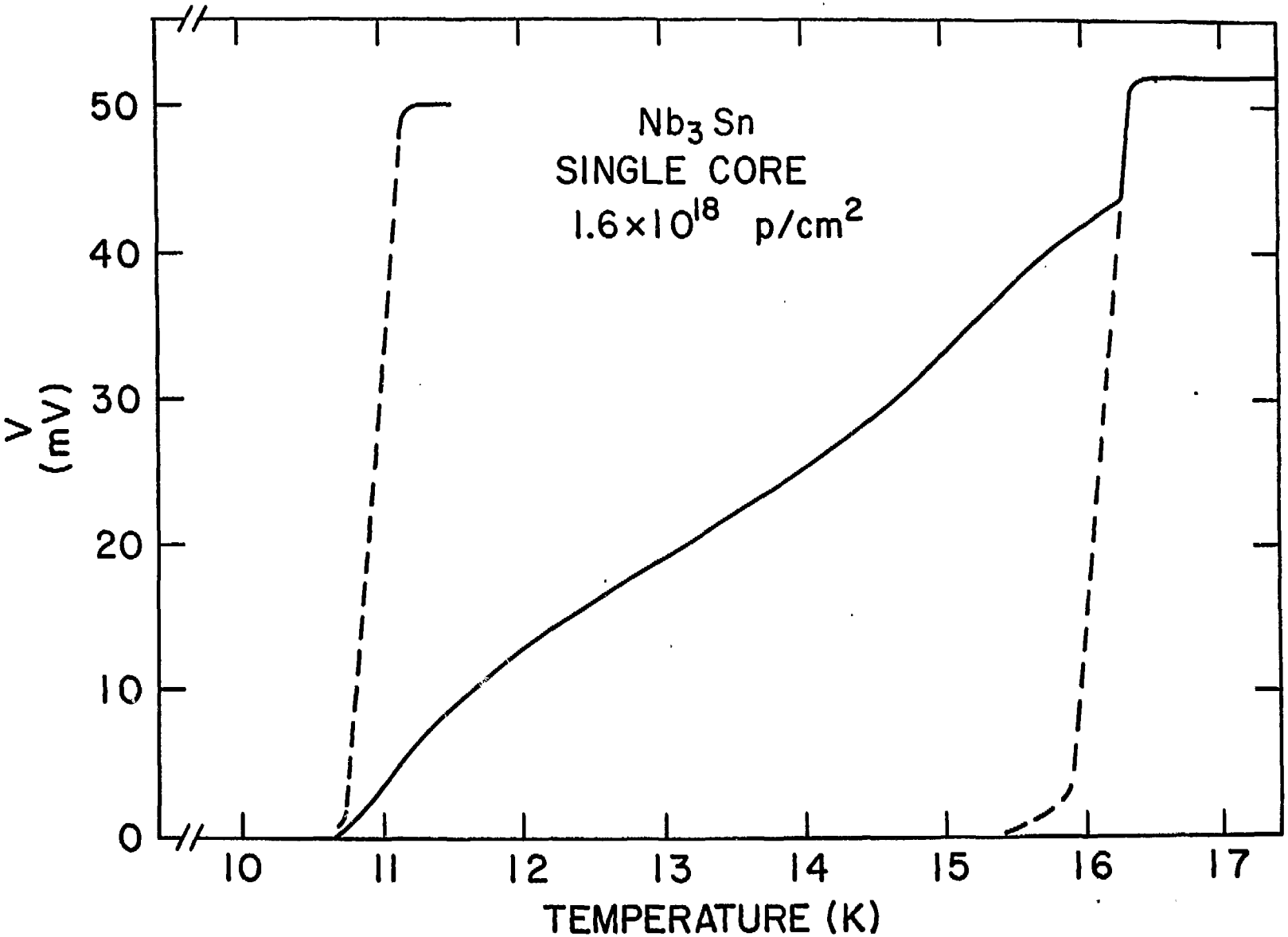
Nb3 Sn
SINGLE CORE
1.6×10^18 p/cm^2
V (mV)
0
10
20
30
40
50
10
11
12
13
14
15
16
17
TEMPERATURE (K)

FIGURE 14.

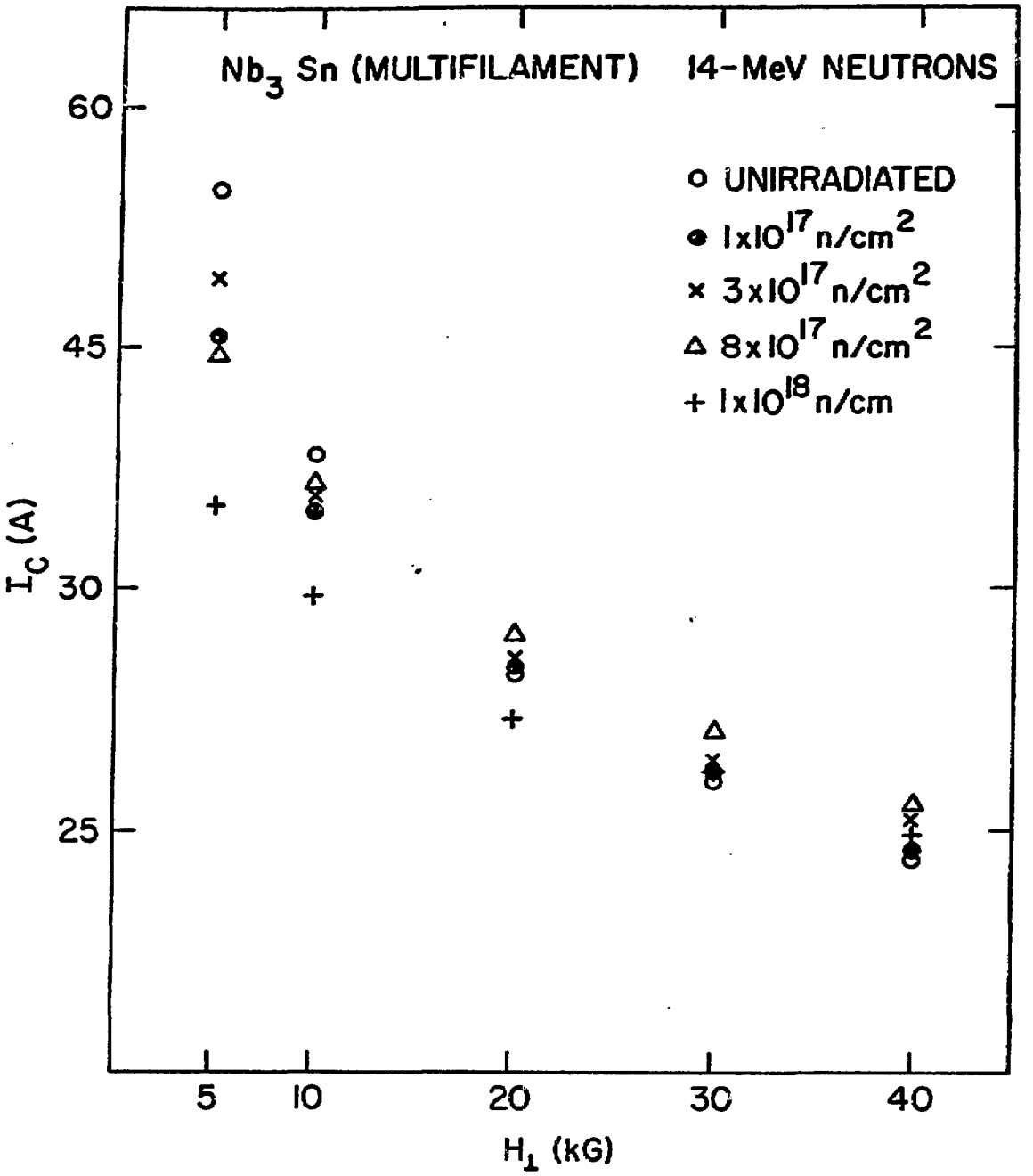
Nb3 Sn (MULTIFILAMENT) 14-MeV NEUTRONS
o UNIRRADIATED
● 1x10^17 n/cm^2
× 3x10^17 n/cm^2
△ 8x10^17 n/cm^2
+ 1x10^18 n/cm
60
45
30
25
Ic (A)
5
10
20
30
40
H⊥ (kG)

FIGURE 15.

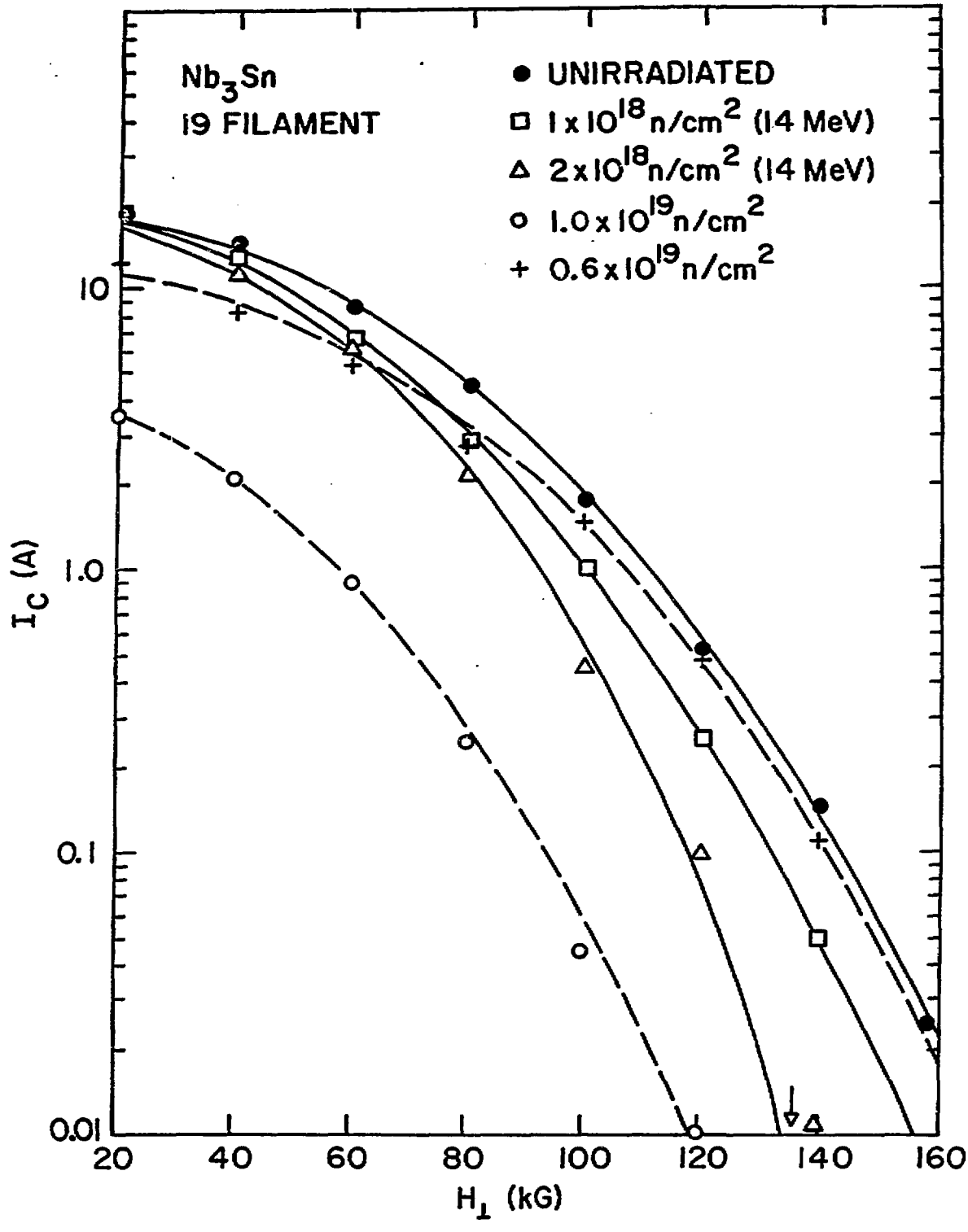
Nb3Sn
19 FILAMENT
UNIRRADIATED
1 x 10^18 n/cm^2 (14 MeV)
2 x 10^18 n/cm^2 (14 MeV)
1.0 x 10^19 n/cm^2
0.6 x 10^19 n/cm^2
Ic (A)
10
1.0
0.1
0.01
20
40
60
80
100
120
140
160
H⊥ (kG)

FIGURE 16.

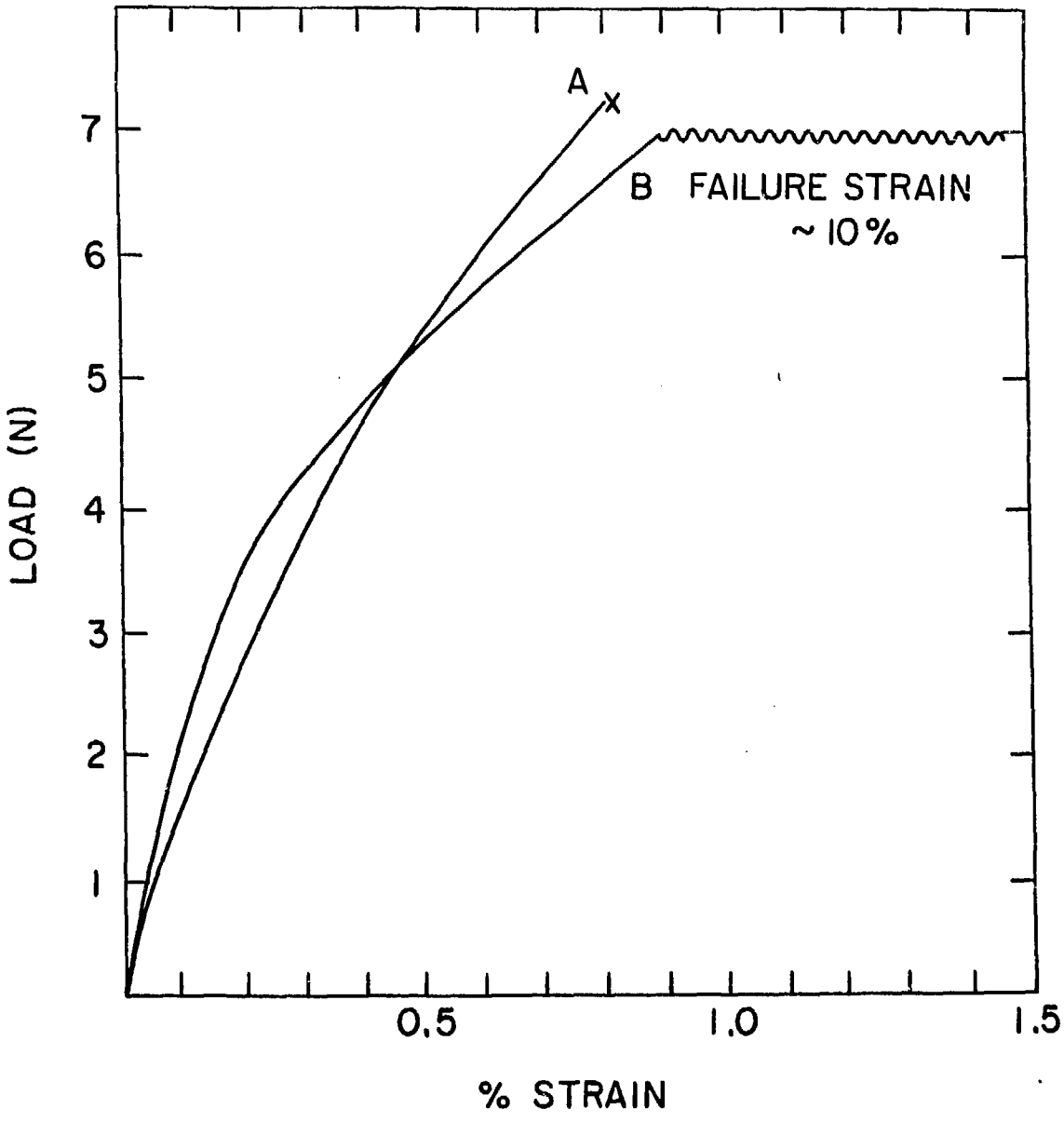

FIGURE 17.

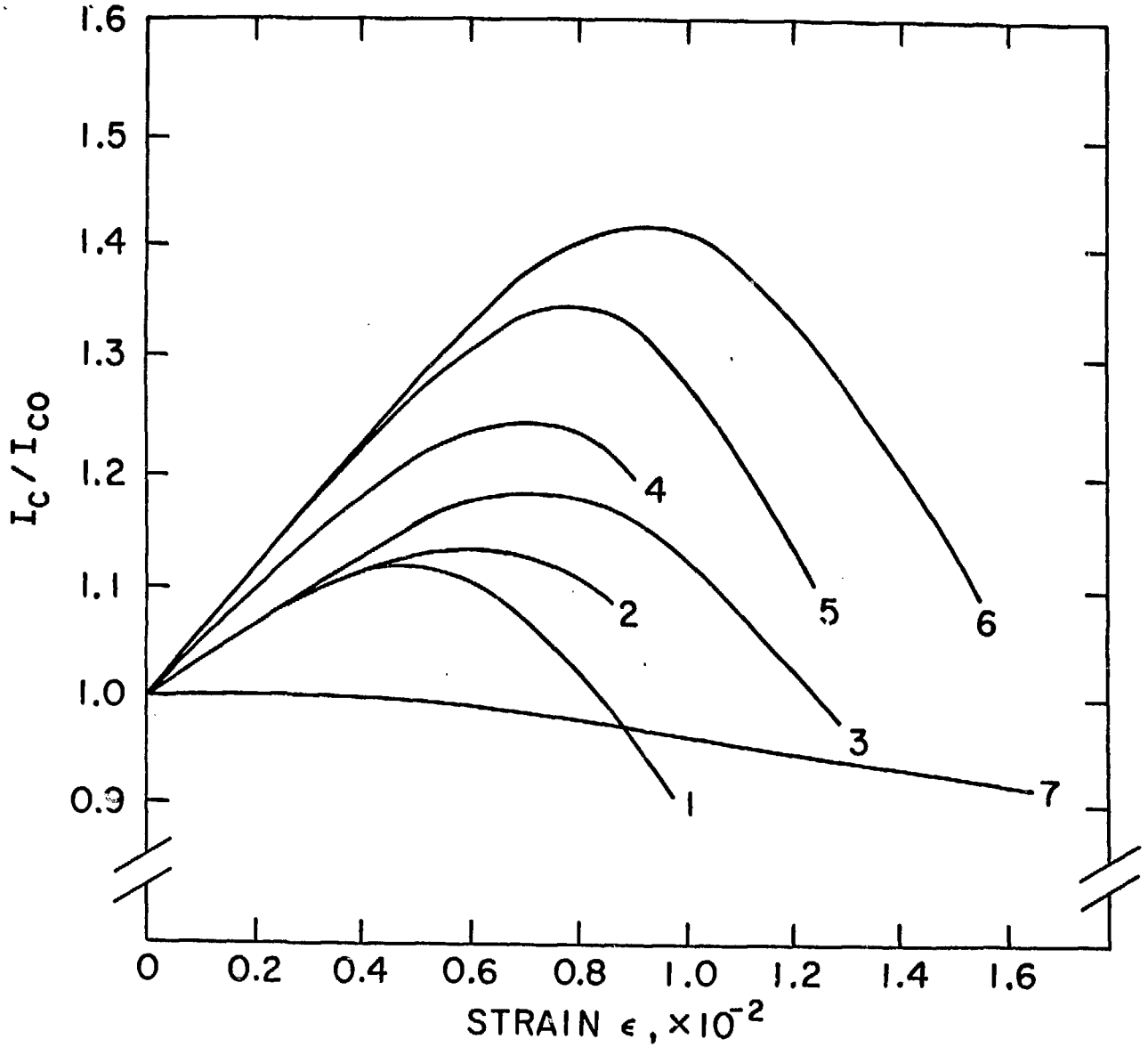
1.6
1.5
1.4
1.3
1.2
1.1
1.0
0.9
I_C / I_{CO}
0
0.2
0.4
0.6
0.8
1.0
1.2
1.4
1.6
STRAIN ϵ, $\times 10^{-2}$
1
2
3
4
5
6
7

FIGURE 18.

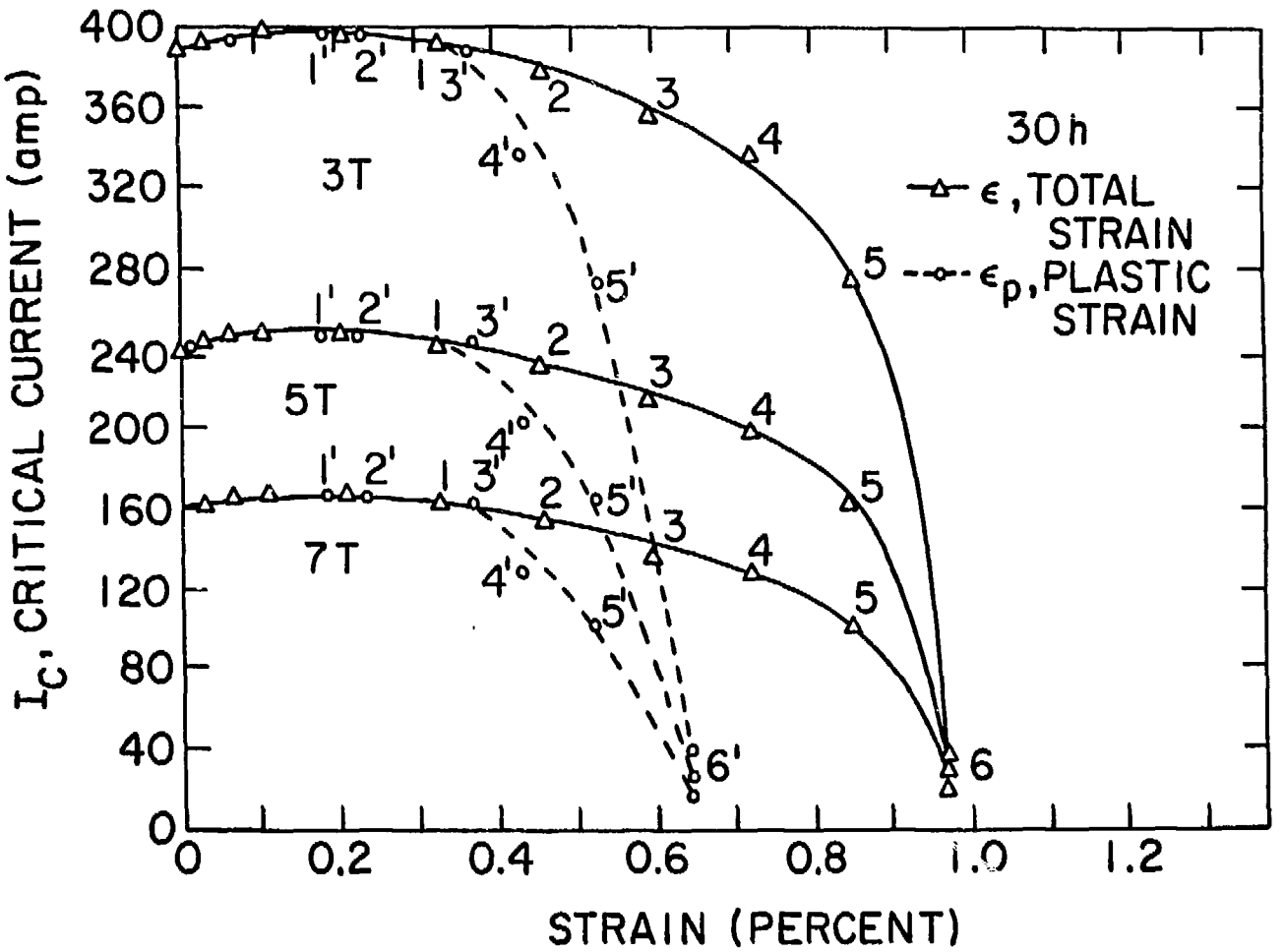
400
360
320
280
240
200
160
120
80
40
0
0
0.2
0.4
0.6
0.8
1.0
1.2
I_c, CRITICAL CURRENT (amp)
STRAIN (PERCENT)
3T
5T
7T
30 h
ϵ, TOTAL STRAIN
ϵ_p, PLASTIC STRAIN
1'
2'
3'
4'
5'
6'
1
2
3
4
5
6

FIGURE 19.

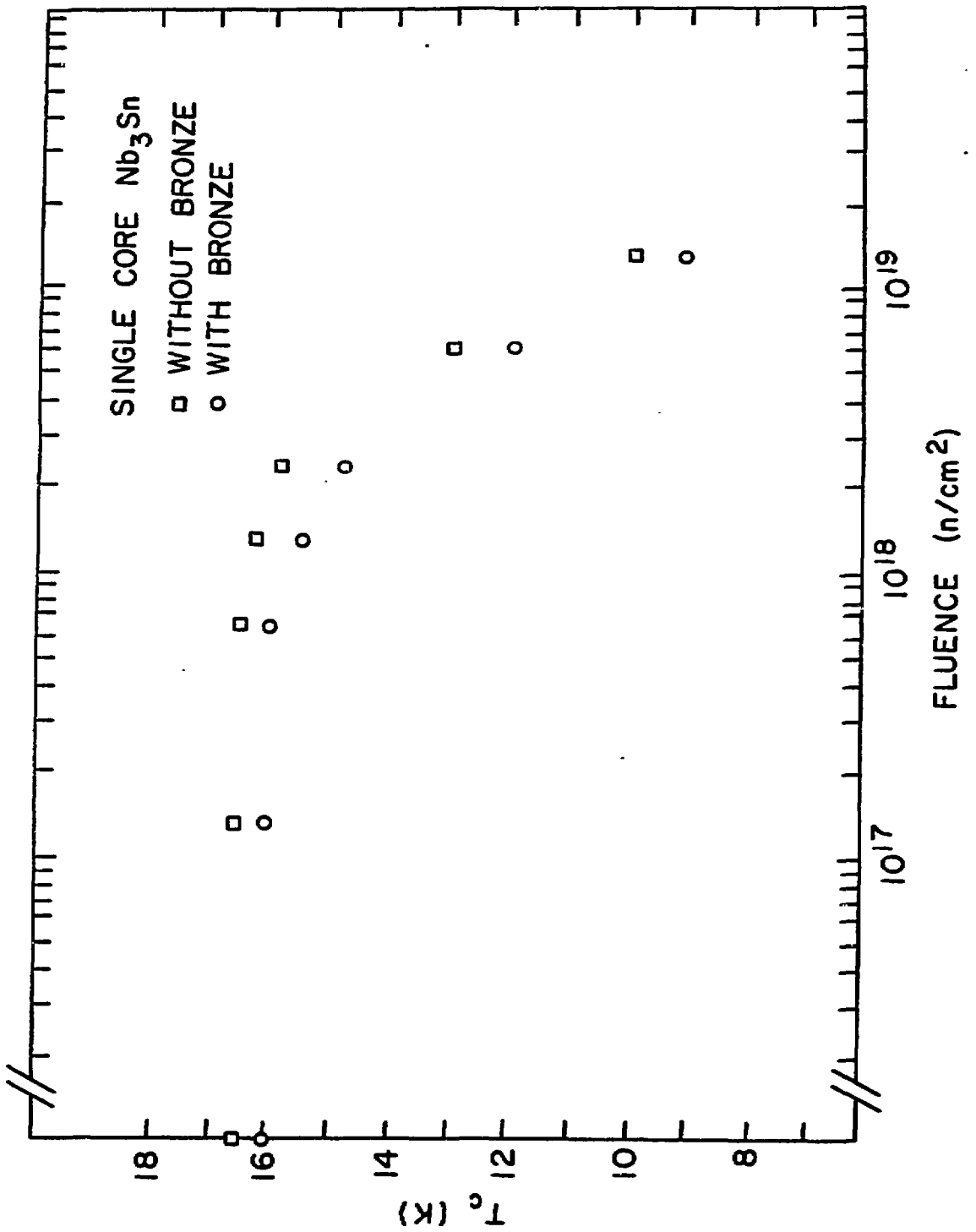
SINGLE CORE Nb_3Sn
□ WITHOUT BRONZE
○ WITH BRONZE
T_c (K)
18
16
14
12
10
8
10^{17}
10^{18}
10^{19}
FLUENCE (n/cm^2)

FIGURE 20.

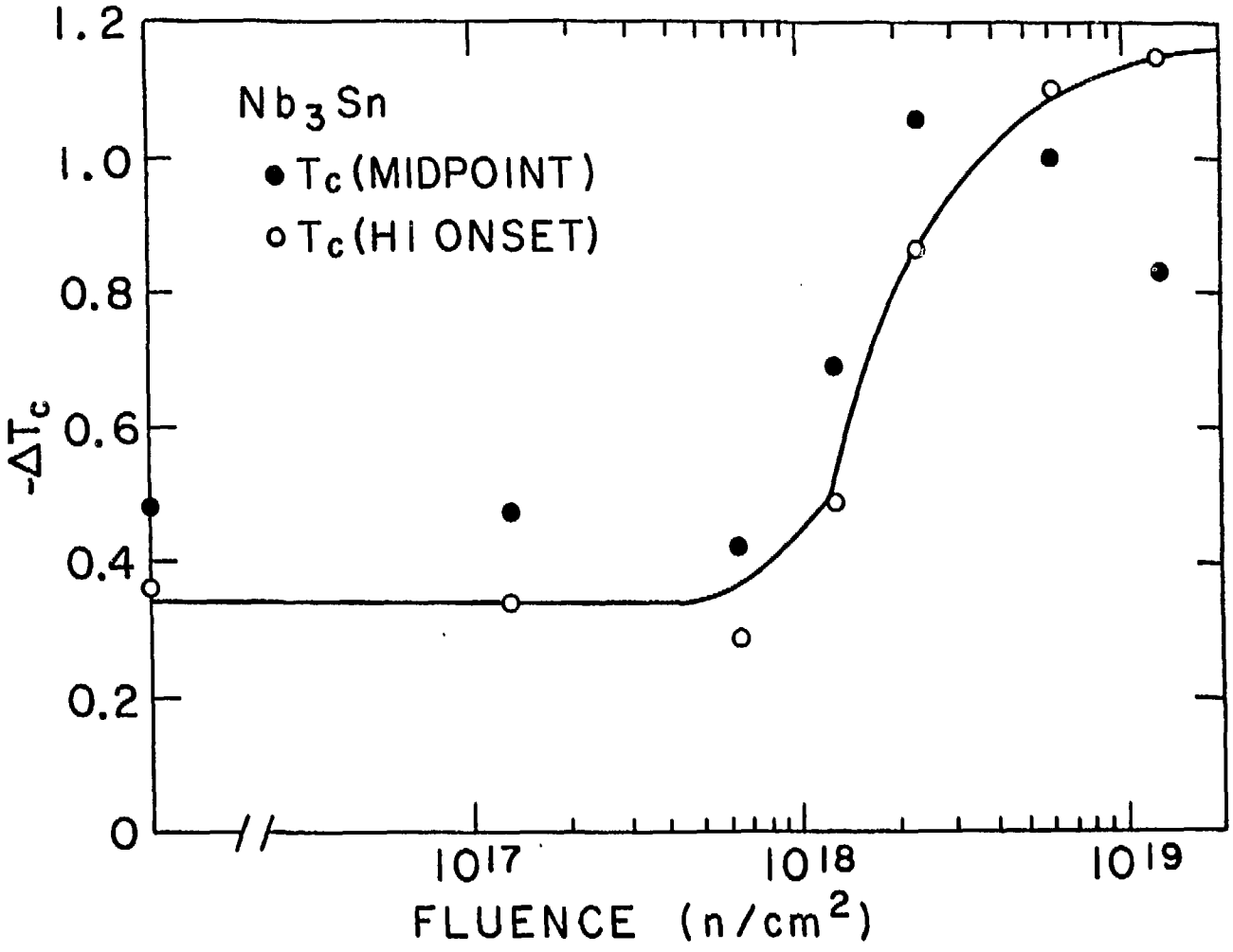
1.2
1.0
0.8
0.6
0.4
0.2
0
$-\Delta T_c$
Nb_3Sn
T_c(MIDPOINT)
T_c(HI ONSET)
10^{17}
10^{18}
10^{19}
FLUENCE (n/cm^2)

FIGURE 21.